NAIST-IS-DD0561042

Doctoral Dissertation

Study on Performance Improvement of ISDB-T Receiver in Fast Fading Environment

Young-Cheol Yu

March 22, 2007

Department of Information Systems
Graduate School of Information Science
Nara Institute of Science and Technology

A Doctoral Dissertation
submitted to Graduate School of Information Science,
Nara Institute of Science and Technology
In partial fulfillment of the requirements for the degree of
Doctor of ENGINEERING

Young-Cheol Yu

Thesis Committee:

Professor Minoru Okada (Supervisor)
Professor Masaki Koyama (Co-supervisor)
Professor Hiroyuki Seki (Co-supervisor)

Study on Performance Improvement of ISDB-T Receiver in Fast Fading Environment*

Young-Cheol Yu

Abstract

Digital terrestrial television broadcasting (DTTB) is attractive both for TV viewers and broadcasters in terms of providing high-definition television (HDTV), multiple stream and additional data transmission services. DTTB viewers can get more information than the traditional analog terrestrial television broadcasting. Currently, DTTB services have already started in major countries including EU nations, the US, South Korea and Japan.

There are a several DTTB standards including European standard, DVB-T (Digital video broadcasting for terrestrial), Japanese one, ISDB-T (Integrated Services Digital Broadcasting for Terrestrial), the US's, ATSC (Advanced Television Systems Committee) and South Korean counterpart, T-DMB (Digital Multimedia Broadcasting for Terrestrial). Among these standards, three standards except for ATSC exploit OFDM (orthogonal frequency division multiplexing) technologies as their physical layer transmission scheme, while ATSC employs 8-level vestigial side band (8-VSB) for its transmission scheme.

OFDM enables high-speed digital transmission over time-dispersive multi-path propagation environment. In OFDM, assigned frequency band is split to a lot of sub-bands, namely, sub-carriers. A high bit rate data stream is divided into a number of low bit-rate streams and transmitted through the corresponding sub-carriers in parallel. In ISDB-T, there are 5617 sub-carriers in one TV channel. Since bandwidth for each sub-carrier is narrow, it does not affect the distortion due to multi-path delay spreading.

*Doctoral Dissertation, Department of Information Systems, Graduate School of Information Science, Nara Institute of Science and Technology, NAIST-IS-DD0561042, March 22, 2007.

However, since the frequency spacing among sub-carriers is narrow, the transmission performance of OFDM can be deteriorated by ICI (Inter-Channel Interference) due to carrier frequency offset (CFO) among transmitter and receiver as well as the Doppler shift due to fast motion of receiver. In ISDB-T, the frequency spacing is only 1kHz , while the Doppler shift reaches 100Hz when the receiver moves at the speed of 150km/h.

The ICI due to CFO and Doppler shift can be compensated by making efficient use of AFC (Automatic Frequency Control). However, in a multi-path environment, each incoming wave is affected by a different Doppler shift, because the incoming waves arrive from different directions. This implies that the received signal is composed of many incoming waves with different Doppler frequencies, namely, Doppler spreading. In this case, the conventional AFC does not work.

To overcome the problem caused by the Doppler spread, a linear array antenna-assisted Doppler spread compensator has been proposed. It estimates the received signal at a fixed position with respect to the ground by making use of linear array antenna followed by the space domain interpolator. However, a linear array antenna-assisted Doppler spread compensator has a drawback in terms of the mutual coupling effect between array elements. The mutual coupling degrades the performance of the Doppler Spread compensator. Polarization mismatching between the transmitter and the receiver is another problem in efficient reception of DTTB signals. In Japan, almost all DTTB stations transmit their signals in horizontal polarization. However, the previously proposed linear array antenna-assisted Doppler spread compensator employs a vertical-polarization monopole array.

In order to solve these problems in a linear array antenna assisted Doppler spread compensator, this thesis firstly proposes a dipole array antenna assisted Doppler spread compensator with maximum ratio combining (MRC) diversity receiver. The mutual coupling effect between array elements is assumed by antenna simulation. Besides, to make use of MRC diversity, the BER (Bit Error Rate) performance is improved in a multi-path fading channel. Computer simulation results showed that the proposed scheme outperforms the conventional scheme.

Next, the thesis proposes dummy elements attached on both sides of monopole array-assisted Doppler spread compensator receiver for overcoming the

mutual coupling problem. Dummy elements, which are terminated with the resistance, are placed at the either ends of linear array antennas in order to compensate for the directivity pattern imbalance due to mutual coupling between elements. Computer simulation results showed that the proposed scheme has wide operating bandwidth and improvement the BER performance of Doppler spread compensator.

Keywords:

Array Antenna, Monopole Array, Dipole Array, Doppler Spread, Mutual Coupling, Dummy Element

List of Publication

Journal Papers

1. Young-Cheol Yu, Minoru Okada, Heiichi Yamamoto, "Dipole Array Antenna Assisted Doppler Spread Compensator with MRC Diversity for ISDB-T Receiver", IEICE Transaction on Communication (Accepted)

2. Young-Cheol Yu, Minoru Okada, Heiichi Yamamoto, "Effect of Dummy Elements on a Monopole Array-assisted Doppler Spread Compensator for a Digital Terrestrial Television Broadcasting Receiver", IEICE Transaction on Communication (Major Revision)

International Conferences (Reviewed)

1. Young-Cheol Yu, Minoru Okada, Heiichi Yamamoto, "Dipole-Array Assisted Doppler Spread Compensator for Mobile Digital Terrestrial Television Broadcasting Receiver", IEEE Radio and Wireless Conference (RAWCON), pp.123 - 126, Atlanta, USA, September 2004.

2. Young-Cheol Yu, Mototsgu Suzuki, Naoki Aoyama, Minoru Okada, Heiichi Yamamoto, "A Simple OFDM Diversity Receiver based on Antenna Combining", IEEE Radio and Wireless Conference (RAWCON), pp.291 - 293, Atlanta, USA, September 2004.

3. Young-Cheol Yu, Minoru Okada, Heiichi Yamamoto, "Dipole-Array Assisted Doppler Spread Compensator with Diversity for Mobile Digital Terrestrial Television Broadcasting Receiver", IEEE Intl. Conference on Consumer Electronics (ICCE), pp.195 - 196, Las Vegas, USA, January 2005.

4. Young-Cheol Yu, Minoru Okada, Heiichi Yamamoto, "Effect of Dummy elements on Monopole-Array assisted Doppler Spread Compensator for Digital Terrestrial Television Broadcasting Receiver", Radio and Wireless Symposium (RWS), pp.203 - 206, San Diego, USA, January 2006.

5. Young-Cheol Yu, Minoru Okada, Kazumichi Andoh, Heiichi Yamamoto, "Dummy Elements Add on Both Sides of Monopole-Array Assisted Doppler

Spread Compensator for Digital Terrestrial Television Broadcasting Receiver", IEEE Intl. Workshop on Antenna Technology : Small Antennas and Novel Metamaterials (IWAT), pp.377 - 380, New York, USA, March 2006.

6. Young-Cheol Yu, Minoru Okada, Heiichi Yamamoto, "Study for Various Array Antenna Assisted Doppler Spread Compensator for ISDB-T Receiver", IEEE 63rd Vehicular Technology Conference-Spring (VTC-Spring) 2006, Vol. 6, pp.2947 - 2951, Melbourne, Australia, May 2006.

7. Young-Cheol Yu, Minoru Okada, Heiichi Yamamoto, "Reactance-Domain Modulation Scheme for Reduction Burst Errors of ISDB-T Receiver in Slow fading Environment", Intl. Symposium on Information Theory and its Applications (ISITA), pp.714 - 716, Seoul, Korea, October 2006.

Domestic Conference

1. Young-Cheol Yu, Mototsuku Suzuki, Minoru Okada, Heiichi Yamamoto, "A Directivity of A OFDM Simple Diversity Receiver", IEICE General Conference, B-1-254, pp.254, Tokyo, March 2004.

2. Young-Cheol Yu, Kazumichi Andoh, Minoru Okada, Heiichi Yamamoto, "Effect of Dummy Elements on Monopole-Array Assisted Doppler Spread Compensator for Digital Terrestrial Television Broadcasting Receiver", IEICE Society Conference, Sapporo, September 2005.

Technical Report

1. Young-Cheol Yu, Minoru Okada, Heiichi Yamamoto, "Dipole-Array Assisted Doppler Spread Compensator with Diversity for Mobile Digital Terrestrial Television Broadcasting Receiver", ITE Technical Report Consumer Electronics, Vol.29, No.21, pp.21-24, March 2005.

2. Kazumichi Andoh, Kim Soo Hwan, Yu Young-Cheol, Minoru Okada, Heiichi Yamamoto, "Effect of Dummy Elements Attached to the Array Assisted Doppler Spread Compensator for Mobile Digital Terrestrial Television

Broadcasting", IEICE Technical Report, vol. 104, no. 677, AP2004-340, pp.221-225, Tokyo, March 2005.

3. Young-Cheol Yu, Minoru Okada, Heiichi Yamamoto, "Study for Various Array Antenna assisted Doppler Spread Compensator with MRC Diversity of ISDB-T Receiver", IEICE Technical Report, Mobile Multimedia Communication (MoMuc), Vol.105, No.264, pp.21-25, September 2005.

Award

1. Mr. Young-Cheol Yu, "IEEE VTS Japan 2006 Young Researcher's Encouragement Award", IEEE Vehicular Technology Society (VTS) Japan Chapter, May 2006.

Acknowledgement

First of all, I would like to express my sincere gratitude to Professor Minoru Okada, who is my supervisor. He provided me with general knowledge in communications theory and practices, as well as fruitful discussion during the Ph.D. course and valuable comments and suggestions during writing this thesis.

I would like to express my gratitude to executive director Heiichi Yamamoto for his guidance and supports during my study at Communications Laboratory, at NAIST.

I would like also to thank my co-supervisor Professor Masaki Koyama for his valuable comments and important suggestions concerning this thesis.

I express my gratitude to Professor Hiroyuki Seki, who is my co-supervisor, for his helpful advice and suggestion concerning this thesis.

I extend my gratitude to Associate Professor Takao Hara and Assistant Professor Masato Saito of Communications Laboratory for their fruitful discussions on related subjects.

I am also greatly indebted to Professor Cheon-Woo Shin and Professor Kwang-Ho Shin, who are in Kyungsung Univ., S.Korea, for getting me interested in Communications. They also gave me advice on how to proceed research.

My sincere thanks to Joji Shimakawa, who is Senior Technology Manager of Philips Japan Ltd., Jos Huisken, who is Chief Silicon Designer of Silicon Hive, for their fruitful discussions and suggestions concerning our co-research and this thesis.

Also, I would like to thank to all students of Communications Laboratory -past and presents- who made my stay at NAIST comfortable and pleasant.

Last, but not least, I thank my family: my parents, sister, my wife and mother in law for unconditional support and encouragement throughout the years.

Contents

List of Figures

List of Tables

Chapter 1

Introduction

Historically, a new technology appeared because the people strongly want to improve the quality of life. Since the advent of new technology, we have been benefited more convenience and efficiency in our life. Thanks to the advent of television, we have obtained more information than the conventional media, radio and newspaper. The earlier television expressed the image only in black and white. As time went by, people wanted to view natural image, namely, colored image. In order to satisfy this requirement, the color television was developed. The television broadcasting technology has further advanced to satisfy our requirement. Now, we are looking forward to appearing a new type of television broadcasting, which can provide interactivity with television and the additional information. The advent of a new type of television broadcasting is now available, because digital transmission and compression technology have rapidly been developed over the last ten years.

A new type of television broadcasting, DTTB (Digital Terrestrial Television Broadcasting) has been started in major countries. DTTB is different from today's "analog" television broadcasting. In analog television broadcasting, the signal is in the form of a continuous wave whereas the signal of DTTB is in the form of discrete bits of information. One of the advantages of digital signal is to detect and restore the errors thanks to the error correction coding technique. Another advantage lies on the capability of reducing the co-channel interference and ghost effect by making efficient use of digital modulation and equalization technologies. Therefore, DTTB can provide more clear and shaper image than the

analog television broadcasting. Furthermore, DTTB provides various services, for example, data broadcasting, electronic program guides (EPGs), interactive services and so on. The viewers are capable of obtaining the additional information through the data broadcasting. By using EPGs, the viewers can navigate between channels, identify the current program and the next program on each channel, provide a short synopsis of the content of programs and search for programs by genre. Moreover, DTTB is capable of improving the frequency efficiency because of advanced digital video compression technologies such are MPEG-2 (Moving Picture Expert Group) and MPEG-4 [1].

One of the DTTB standards, ATSC (Advanced Television Systems Committee) [2], was adopted on December 24, 1996 in the US. ATSC is intended to replace the conventional analog TV system, national television systems committee (NTSC) without major changes in existing analog television transmitter. Therefore, ATSC was designed to permit an additional digital transmitter to be added to each national television systems committee (NTSC) transmitter. ATSC employs 8-VSB modulation as a physical layer transmission scheme and it occupies 6MHz frequency bandwidth, which is the same as for the conventional TV system. The information bit rate by ATSC is up to 19.39Mbit/s, which is sufficient to carry a high definition video and audio stream with meta-data. Moreover, numerous auxiliary data casting services can be provided. ATSC is also adopted by Canada, Mexico and South Korea.

In Europe, DTTB standard, DVB-T (Digital Video Broadcasting for Terrestrial) [3], was standardized in 1997. The first DVB-T service was started in the United Kingdom in 1998. DVB-T employs OFDM (Orthogonal Frequency Division Multiplex) for its transmission scheme, it is robust against interference due to multi-path delay spreading. Moreover, single frequency network (SFN), or, all the relay stations that transmit the same program can share one TV channel, can be established since OFDM is robust to the distortion due to delay spreading. Furthermore, in contrast to ATSC, DVB-T is capable of adopting various environments by changing its transmission parameters. Broadcaster can select the transmit parameters such as, modulation format, the code rate and guard interval, according to channel conditions and performance requirements. The bit rate is 16.58 Mbit/s, when a broadcaster selects 16 QAM (Quadrature Ampli-

tude Modulation), code rate is 2/3 and the guard interval is set to 1/8 of OFDM observation interval. The occupied bandwidth can be adjusted into 6, 7 or 8 MHz in order to match TV frequency plans in several countries. The frequency spacing among TV channels in the Europe is 8MHz while the countries employing NTSC as an analog TV standard uses 6MHz spacing. In some Asia and pacific countries such as Australia employs the frequency spacing of 7MHz. DVB-T can be deployed to all the countries despite of frequency spacing. Many European countries are now trying to fully replace the analog TV services by DTTB by 2010.

In Japan, another standard was employed as DTTB service. On December 2003, DTTB service based on ISDB-T (Integrated Services Digital Broadcasting for Terrestrial) [4], was started. It employs OFDM for its transmission scheme as well as DVB-T. There are 5617 sub-carriers in one ISDB-T channel and these sub-carriers are devided into 13 frequency segments. Each segment is composed of 432 sub-carriers. Thanks to the segment structure, ISDB-T provides hierarchical transmission sub-band reception for handheld terminals. Broadcasters select transmission parameters including modulation format and error correction coding rate, on a segment-by-segment basis. ISDB-T provides HDTV and multi-channel SDTV within 6 MHz bandwidth. Furthermore, the transmitted signals for stationary and mobile reception services can be combined in transmission by means of the hierarchical layers. One segment in the center of bandwidth can be independently transmitted as audio and data services for partial reception by portable receivers or mobile phone. Also, ISDB-T has robustness against multi-path and propagation fading. Moreover, building up SFN is possible so as to make more effective use of radio frequency. Japanese government announced that all the terrestrial television services become digital on July 2011.

In South Korea, another standard, digital terrestrial television broadcasting for terrestrial T-DMB (Digital Multimedia Broadcasting for Terrestrial) [5] was introduced for television for mobile terminals. T-DMB also employs OFDM.

One of the major problems in DTTB is multi-path propagation. In order to solve this problem, three major DTTB standards, DVB-T, ISDB-T, and T-DMB employs OFDM as mentioned above.

OFDM is a promising technique capable of transmitting broadband digital

stream in time-dispersive multi-path propagation environment. In OFDM, a single data-stream to be transmitted is divided into a number of lower rate streams and transmitted by modulating corresponding sub-carriers. Since the bandwidth of each sub-carrier is narrow enough to neglect the time-dispersion due to multi-path, OFDM is robust against frequency selectivity of the multi-path propagation channel as well as narrow band interference. Therefore, many wireless communication standards adopt OFDM for its physical layer transmission scheme such as wireless local area network (W-LAN) standards, IEEE (Institute of Electrical and Electronics Engineers) 802.11a and 802.11g [6], and broadband fixed wireless access IEEE 802.16 also referred to as WiMAX (Worldwide Interoperability for Microwave Access), other than DTTB. However, because of the narrow bandwidth among sub-carriers, OFDM is sensitive to inter-channel interference (ICI) due to Doppler shift and carrier frequency offset (CFO) between the transmitter and receiver. In ISDB-T, the target of this thesis, the bandwidth among sub-carriers is only about 1kHz. On the other hand, the Doppler shift reaches 100Hz when the receiver on vehicle moves at the speed of 150km/h assuming that the operating frequency is 770MHz. Furthermore, the frequency accuracy of the commercial grade local oscillator in the receiver side is around 10 ppm. That is, CFO could reach 10kHz. This implies that ICI due to CFO and Doppler shift could deteriorate the reception performance.

In multi-path propagation environment, several paths are arriving toward the receiver from the different direction, and each path affects the different Doppler shift according to the direction of arrival. The received signal is the sum of the multiple paths with different Doppler shift frequencies. In the following, this phenomenon is referred to as "Doppler spread". The ICI due to CFO and Doppler shift may be solved by making use of automatic frequency control (AFC). However, AFC does not work when it encounters Doppler spread.

There are many studies to overcome the problem on Doppler spread effect. In [7], the authors described CFO estimation based on frequency domain training sequence. According to the reference [7], transmitter needs training sequence for reducing frequency offset. However, we could not apply this scheme to ISDB-T receiver, because the transmitted signal does not have frequency domain training sequence. On the other hand, the directional antenna based scheme for reduc-

ing Doppler spread effect has been proposed [8]. In this method, the directional antennas are installed on top of a vehicle, the incoming waves are divided into a several paths according to their directions of arrival. The Doppler spread of the output signal from each directional antenna becomes smaller than that of omni-directional antenna since the directions of arrival are limited by directivity of antennas. That is, the Doppler effect of each directional antenna can be compensated for by the conventional AFC. However, this method has a major drawback in terms of its size of antennas. Meanwhile, another type of Doppler spread compensation algorithm has been proposed [9]. S.A. Husen and S. Baggen proposed the ICI canceller in frequency domain. The received signal is first decomposed to the OFDM sub-channel components and interference, due to Doppler spread, is cancelled by a frequency domain Wiener filter. Although it requires only one antenna, its signal processing part requires huge complexity.

A linear array antenna assisted Doppler spread compensator has been proposed by Okada et al [10] in order to overcome the drawbacks of the conventional schemes mentioned above. In this method, Doppler spread compensator estimates the received signal at a fixed point with respect to the ground by making use of the received signals from several array elements followed by a space domain interpolator. According to the results of bit error rate (BER) performance, a linear antenna assisted Doppler spread compensator is possible to mitigate Doppler spread effect. In this thesis, this Doppler spread compensator is called the "conventional" scheme.

Although the conventional Doppler spread compensator is an efficient anti-Doppler spread compensation technique, it has several drawbacks. One is the polarization mismatching between the transmitter and receiver. In Japan, almost all ISDB-T stations transmit their signals in horizontal polarization. In order to receive ISDB-T signals efficiently, the receiver should be needed horizontally-polarized antenna. However, the conventional scheme uses a vertical-polarization monopole array. The polarization mismatch loss between the transmitter antenna and receiver antenna can degrade the received signals strength. Another problem is the mutual coupling effect among array elements. The mutual coupling effect is caused due to narrow antenna spacing among array elements. This mutual coupling changes radiation pattern of each array element. In this case, the con-

ventional Doppler spread compensator is difficult to estimate the received signals at a fixed position with respect to the ground. Therefore, the performance of Doppler spread compensator deteriorates due to mutual coupling.

To reduce the mutual coupling effect, the proposed Doppler spread compensator has employed a mutual coupling canceller [10, 11], which calculates a mutual impedance matrix normalized by the load impedance. Hence, the mutual coupling canceller is sensitive to changes of carrier frequency. Moreover, its operating bandwidth is narrow compared with the television frequency band [10, 11]. For reference, the carrier frequency of ISDB-T is from 470MHz to 770MHz, and its bandwidth is 300MHz.

First, to solve polarization mismatch loss, I propose a dipole array antenna assisted Doppler spread compensator with maximum ratio combining (MRC) diversity receiver. To use dipole array, polarization mismatch loss can be reduced. Besides, to make use of MRC diversity, the BER performance can be improved in a multi-path fading environment. By making use of antenna simulation, I assumed mutual coupling effect between each array element.

Second, to reduce mutual coupling effect among array elements, dummy elements method is already proposed [12, 13]. In [12], dummy elements are terminated with matched loads on each side of array to provide a similar environment for all the inner array elements. This method is a simple way to reduce mutual coupling effect. However, it needs more space to set the arrays and more elements. In this thesis, I use dummy elements, which are attached on both sides of monopole array. Dummy elements can be reduced the mutual coupling effect between main elements because dummy elements are coupling with main elements. That is, dummy elements can disperse the mutual coupling effect between main elements. Therefore, the BER performance of Doppler spread compensator can be improved.

The rest of this thesis is organized as follows. Chapter 2 describes the world DTTB standards, for example, ISDB-T, DVB-T and T-DMB. Also, transmission scheme of DTTB, OFDM, will be explained. Chapter 3 describes impact of Doppler shift on the BER performance of OFDM system. Chapter 4 presents the solution of polarization mismatch loss, which is dipole array assisted Doppler spread compensator with MRC diversity receiver. The numerical results show

the effectiveness of proposed scheme. Chapter 5 gives the solution of mutual coupling effect between main elements, which is dummy elements add on both sides of monopole array assisted Doppler spread compensator. The antenna simulation results and numerical results prove that dummy elements method can reduce the mutual coupling and also it can improve performance of Doppler spread compensator. Chapter 6 concludes this thesis.

Chapter 2

Digital Terrestrial Television Broadcasting Standard

2.1. Introduction

Figure 2.1 shows the present DTTB standards adaptation status of the world. In the US, they adopted ATSC [2] for their DTTB standard. The European DTTB standard is DVB-T [3] and the Japanese one is ISDB-T [4]. Also, the Korean adopts ATSC for stationary reception and T-DMB [5] for mobile reception.

Except for ATSC, DVB-T, ISDB-T and T-DMB employ OFDM for their transmission scheme. On the other hand, ATSC employs 8-VSB for its transmission scheme. ATSC has advantage at the stationary reception and it is possible to provide high-speed transmission rate. However, ATSC has weakness in mobile environment because ATSC exploits single carrier to transmit the signal. It means that single carrier is easily deteriorated by frequency selective fading and multi-path delay spread. In contrast, the other DTTB standards, which employ OFDM, have advantage in mobile environment. OFDM is robust multi-path delay spread because it has guard interval. Also, in frequency selective fading environment, several sub-carriers among a number of sub-carriers are only deteriorated.

This chapter gives a principle of OFDM followed by an overview of OFDM based on DTTB standards, ISDB-T, DVB-T and T-DMB.

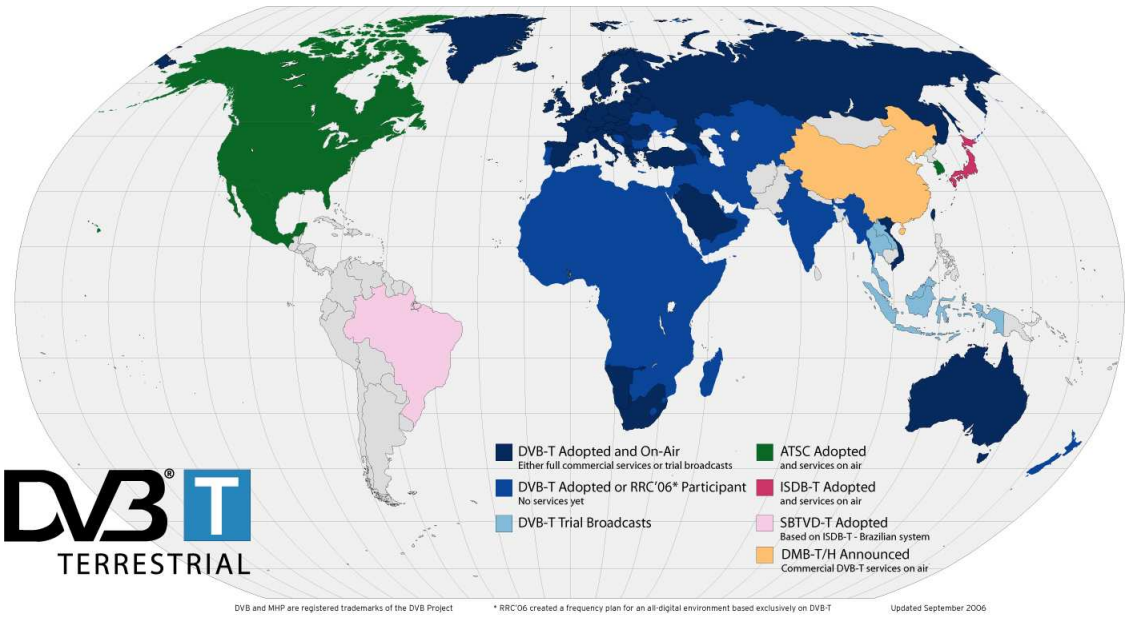

Figure 2.1. The present DTTB standards adaptation status of the World [14]

2.2. Orthogonal Frequency Division Multiplexing (OFDM)

2.2.1 Principle of OFDM

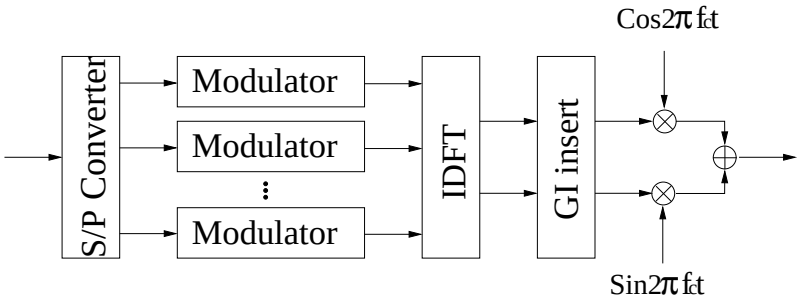

Figure 2.2. Diagram of OFDM Transmitter

Since OFDM transmits a single data stream on a number of lower rate sub-carriers, OFDM is the efficient way to handle multi-path propagation. In

particular, it has robustness against frequency selective fading or narrow band interference. In a single carrier system, a single fade or interferer can cause the entire link to fail, but in OFDM, only a small percentage of the sub-carriers will be affected [15].

Figure 2.2 shows the block diagram of OFDM transmitter. First digital data stream is divided into several sub-streams by S/P converter (Serial to Parallel converter). Then the divided data streams are modulated by digital modulators. Hence, the modulated signals are applied to IDFT(Inverse Discrete Fourier Transform) block. GI (Guard Interval) signal is added to the output signals of IDFT. By adding guard interval to OFDM signals, it can remove inter-symbol interference. OFDM signals are transformed to RF(Radio Frequency) signals by local oscillator having frequency of f_c and then transmitted from the antenna.

Figure 2.3 shows diagram of OFDM receiver. First, received RF signals are down-converted in its frequency by the orthogonal demodulators and the equivalent low pass signal is generated. Then, the guard interval is removed from the signal. Baseband signals are transformed to the sub-channel components by DFT (Discrete Fourier Transform) unit. The outputs of DFT are applied to the one-top equalizers (EQ) followed by the digital demodulator. At the one-top equalizers, the amplitude and phase shifts due to multi-path propagation channel are compensated. The demodulators restore the digital data streams from QAM symbols. Finally, P/S converter (Parallel to Serial converter) re-orders the sub-channel streams into the original high bit rate stream.

The OFDM transmission scheme has the following key advantages: [15]

1. OFDM is an efficient way to deal with multi-path; for a given delay spread, the implementation complexity is significantly lower than that of a single carrier system with an equalizer.

2. In relatively slow time-varying channels, it is possible to significantly enhance the capacity by adapting the data rate per sub-carrier according to the signal-to-noise ratio of that particular sub-carrier.

3. OFDM is robust against narrow band interference, because such interference affects only a small percentage of the sub-carriers.

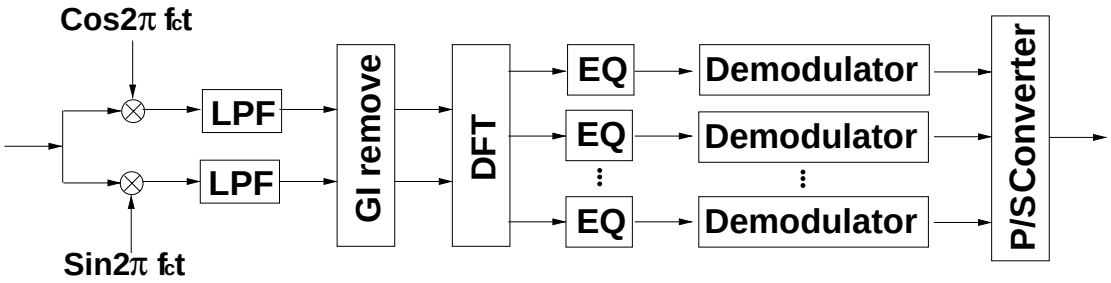

Figure 2.3. Diagram of OFDM Receiver

4. OFDM makes single-frequency networks (SFN) possible, which is especially attractive for broadcasting applications.

On the other hand, OFDM also has some drawbacks compared with single carrier modulation:

1. OFDM is more sensitive to frequency offset and phase noise.
2. OFDM has a relatively large peak-to-average power ratio (PAPR), which tends to reduce the power efficiency of the RF amplifier.

2.2.2 Modulation of OFDM Signals

Let us assume that the QAM symbol corresponding to the nth of sub-carrier is

$$u_n = u_{nI} + ju_{nQ} \tag{2.1}$$

where u_{nI} and u_{nQ} indicate that the inphase and quadrature components of the $n-th$ QAM symbol, respectively. According to Equation (2.1), OFDM signals, which combine with $n = 0 \sim N-1$ of baseband OFDM signals, transmitted simultaneously within period T.

The RF OFDM signal is given by

$$S_{RF}(t) = Re\Big[e^{j2\pi f_c t} \cdot S_{OFDM}(t)\Big] \tag{2.2}$$

Then the baseband OFDM signal, also, is defined by:

$$\begin{aligned} S_{OFDM}(t) &= \sum_{n=-M}^{M} u_n e^{j2\pi n f_0 t} \\ &= \sum_{n=-M}^{M} u_n e^{j2\pi n f_0 t/T_0} \end{aligned} \tag{2.3}$$

wheref_0 is the frequency spacing amongst sub-carriers, and $T_0 = 1/f_0$ is the window period.

The number of sub-carrier is given by

$$N_s = 2M + 1 \tag{2.4}$$

Let us assume that the real and imaginary component of $S_{OFDM}(t)$ are $S_I(t)$ and $S_Q(t)$, respectively. Then Equation (2.2) can be revised as

$$\begin{aligned} S_{RF}(t) &= Re[(S_I(t) + jS_Q(t))(cos2\pi f_c t + jsin2\pi f_c t)] \\ &= S_I(t)cos2\pi f_c t - S_Q(t)sin2\pi f_c t \end{aligned} \tag{2.5}$$

At the receiver, the received signal is transformed to the baseband signal again by multiplying the RF sinusoidal signal generator by local oscillator. LPF (Low Pass Filter) is needed by removing high frequency component which produced by down converting process. Let r_{RF} be the RF received signal. The base band received signal is given by

$$\begin{aligned} r(t) &= r_{RF} \cdot e^{-j2\pi f_c t} \\ &= r_{RF}cos2\pi f_c t - jr_{RF}sin2\pi f_c t \end{aligned} \tag{2.6}$$

$r(t)$ is then applied to FFT processor where discrete Fourier transformation is performed. The revised symbol at the $n-th$ sub-carrier is given by

$$v_n(t) = \frac{1}{T_0}\int_0^{T_0} r(t)e^{-j2\pi nt/T_0}dt \tag{2.7}$$

The AWGN (Additive White Gaussian Noise) channel, that is, assume the re-

ceived signal is distributed by the AWGN. Then the received signal is given by

$$r(t) \;=\; h \cdot S_{OFDM}(t) + z(t) \tag{2.8}$$

where h is the propagation path loss factor and zt is the complex-Gaussian noise component. Substituting the Equation (2.8) in to Equation (2.7),

$$\begin{aligned} v_n &= \frac{1}{T_0}\int_0^T h \cdot S_{OFDM}(t) e^{-j2\pi nt/T_0} dt + \frac{1}{T}\int z(t) e^{-j2\pi nt/T_0} dt \\ &= h \cdot \frac{1}{T_0}\int_0^{T_0} \{\sum u_k e^{j2\pi kt/T_0}\} e^{-j2\pi nt/T_0} dt + z_n \\ &= h \cdot u_n + z_n \end{aligned} \tag{2.9}$$

where,

$$z_n \;=\; \frac{1}{T_0}\int z(t) e^{-j2\pi nt/T_0} dt \tag{2.10}$$

is the noise component corresponding to the $n-th$ sub-carrier.

2.2.3 Guard Interval

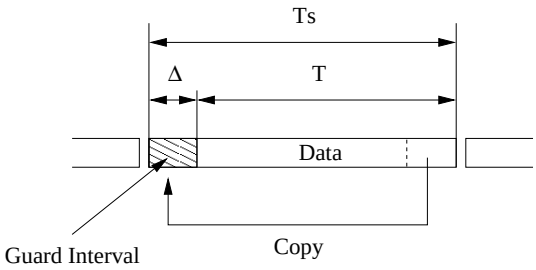

Figure 2.4. Insert Guard Interval

One of the most important reasons to employ OFDM is its robust feature against multi-path delay spread [15]. The symbol duration is made N_s times than the original stream by dividing the input data stream in N_s sub-carriers, which reduces the relative multi-path delay spread, relative to the symbol time, by the same factor. A guard interval is introduced for each OFDM symbol to eliminate

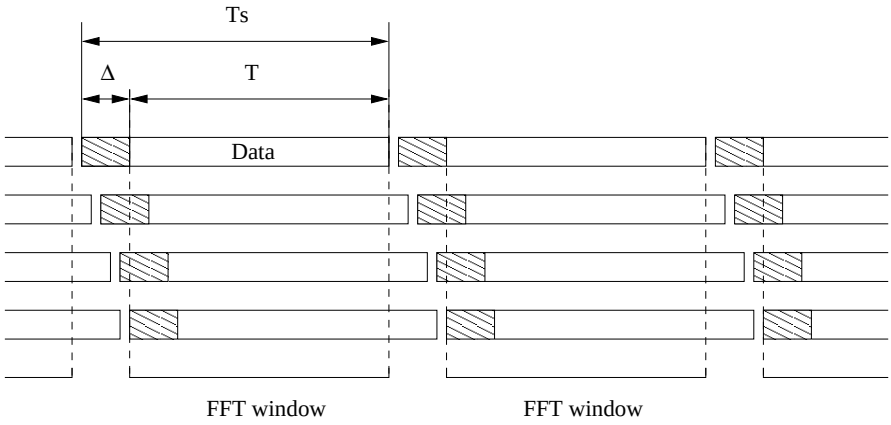

Figure 2.5. Effect of Guard Interval

inter-symbol interference. Hence, the guard interval is selected larger than the expected delay spread, as multi-path delay from one symbol cannot interfere with the next symbol.

Figure 2.4 shows the addition of the guard interval. Δ indicates the length of the guard interval and T_0 is effective symbol duration it is also same as FFT window size. $T_s = \Delta + T_0$ is OFDM symbol time. When Δ is chosen to be larger than the delay spreading, ISI (Inter Symbol Interference) can be removed, as shown in Figure 2.5. During the guard interval, the tail part of the window interval is retransmitted, in order to remove the ICI effect due to multi-path delay spreading.

Firstly, let us assume that the zero is padded during the guard interval, and received signal. The OFDM signal is then given by

$$S_{OFDM} = \begin{cases} \sum u_n e^{j2\pi nt/T_0} & 0 \leq t < T_0 \\ 0 & -\Delta \leq t < 0 \end{cases} \tag{2.11}$$

When the received signal is delayed at τ, the received signal is given by

$$r_{OFDM}(t) \quad = \quad S_{OFDM}(t - \tau) \tag{2.12}$$

where the additive noise component and propagation path loss factor are removed

in order to simplify the discussion. Substituting the Equation (2.12) into the Equation (2.7), we can get the following equation:

$$\begin{aligned} v_n &= \frac{1}{T_0}\int_0^T r_{OFDM}(t)e^{-j2\pi nt/T_0}dt \\ &= \frac{1}{T_0}\int_0^{T_0}\{\sum_k u_k e^{j2\pi k(t-\tau)/T_0}\}e^{-j2\pi nt/T_0}dt \\ &= \sum_k \frac{u_k}{T_0}e^{-j2\pi k\tau/T_0}\cdot\int_\tau^{T_0} e^{j2\pi(k-n)t/T_0}dt \\ &= \sum_k u_k e^{-j2\pi k\tau/T_0}\cdot\{\frac{1}{T_0}\int_0^{T_0} e^{j2\pi(k-n)\tau/T_0}dt - \frac{1}{T_0}\int_0^{\tau} e^{j2\pi(k-n)t/T_0 dt}\} \\ &= u_n e^{-j2\pi n\tau/T_0} - \sum_k u_k e^{-j2\pi k\tau/T_0}\cdot e^{-j2\pi(k-n)\tau/T_0}\cdot(\frac{\tau}{T_0})sinc\{(k-n)\frac{\tau}{T_0}\} \end{aligned} \tag{2.13}$$

where,

$$sinc(x) = \frac{sin\pi x}{\pi x} \tag{2.14}$$

In Equation 2.13, the first term represents the desired symbol component ant the second term corresponds to the interference from the adjacent subchannels. In the following this interference is referred to as "ICI (Inter-Channel Interference)".

In order to cancel ICI, the tail of the DFT waveform is copied to the guard interval. In the following, this signal is called cyclic extension. The transmitted signal is now given by

$$S_{OFDM} = \begin{cases} S_w(t) = \sum u_n e^{j2\pi nt/T_0} & 0 \le t < T_0 \\ S_w(t-T_0) = \sum u_n e^{j2\pi n(t-T_0)/T_0} = \sum u_n e^{j2\pi n(t-T_0)/T_0} & -\Delta \le t < 0 \end{cases} \tag{2.15}$$

This can futher be simplified to

$$S_{OFDM} = \Big\{ S_w(t) = \sum u_n e^{j2\pi nt/T_0} \quad -\Delta \le t < T_0 \tag{2.16}$$

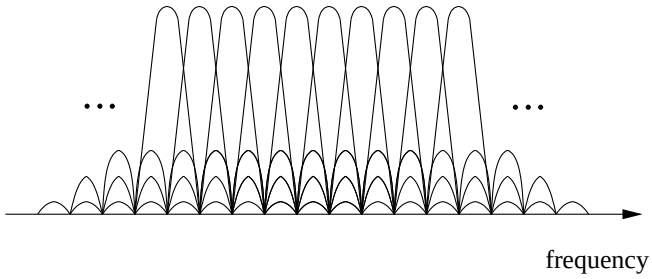

Figure 2.6. Spectrum of OFDM signals:Add the Null data to The Guard Interval

The received signal is again delayed by τ. The output of the FFT is then given by

$$\begin{aligned} v_n &= \frac{1}{T_0}\int_0^T r_{OFDM}(t)dt \\ &= \frac{1}{T_0}\int_0^T S_{OFDM}(t-\tau)dt \\ &= u_n e^{-j2\pi n\tau/T_0} \end{aligned} \tag{2.17}$$

This equation shows that there is no ICI thanks to the cyclic extension

Although the guard interval is setting advisable for as long as multi-path delay, it is unnecessary signal when OFDM receiver demodulate OFDM signal. Accordingly, consideration of propagation environment is needed when decide the guard interval. In the case of ISDB-T, it can be chosen from 1/4, 1/8, 1/16, 1/32 of effective symbol duration.

Moreover, the guard interval can be used frequency synchronization and symbol timing. OFDM signals are delayed as effective symbol duration time then calculated correlation of each symbol. To synchronize symbol and frequency, we should detect a peak value, which is obtained from correlation results.

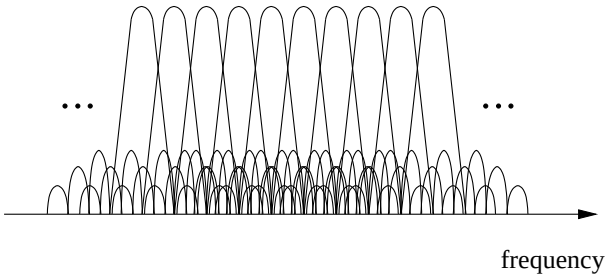

Figure 2.7. Spectrum of OFDM signals:Add the cyclic prefix to The Guard Interval

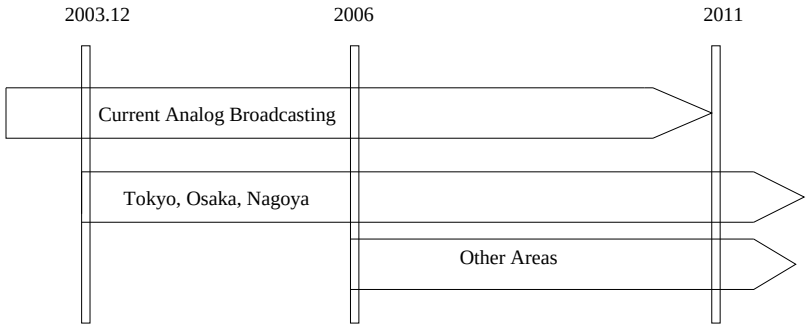

Figure 2.8. Schedule of ISDB-T

2.3. ISDB-T

2.3.1 What is ISDB-T?

ISDB-T began in the three metropolitan areas of Tokyo, Osaka and Nagoya on December 2003. The Japanese government's plan describes a schedule for ISDB-T to have started in all major cities by the end of 2006, and for current analog broadcasting to have been completely replaced with digital broadcasting by 2011. Also, for mobile reception, ISDB-T 1segment broadcasting has already started on April 2006. The characteristics of ISDB-T are as follows [16]:

1. HDTV and multi-channel SDTV can be provided within 6MHz bandwidth.
2. Advanced broadcasting services, such as multimedia and interactive services can be provided.

3. ISDB-T is available in mobile reception.

4. Signals for fixed and mobile reception services can be combined in transmission by means of the hierarchical layers.

5. Robustness against multi-path (ghost) and fading can be obtained.

6. One segment in the center of bandwidth can be independently transmitted as audio and data services for partial reception by portable receivers.

7. Building up Single Frequency Networks (SFN) is possible so as to make more effective use of radio frequency.

8. Compatibility with digital terrestrial sound broadcasting system can be obtained.

2.3.2 Technical Aspect of ISDB-T

The bandwidth of ISDB-T signal is chosen to be 5.6MHz in order to match the existing analog television channel plan, in Japan. The total bandwidth is separated to 13 segments, each of which has 430kHz in bandwidth. Thanks to this segment structure, ISDB-T provides various type of broadcasting including HDTV, SDTV, sound, graphics, text and so on. Since it contains a variety of broadcasting contents, the ISDB-T system should cover a wide range of requirements that may differ from one to another. For example, a large transmission capacity is required for HDTV service which used all 13 segments for transmission and SDTV uses 4 segments it transmitted the other 3 programs at the same time. Moreover one segment, located at the center of the segments, is dedicated for transmitting low-profile video streams. ISDB-T standard employs hierarchical transmission and partial reception to conform this requirement.

Figure 2.9 shows the block diagram of the ISDB-T transmitter. Firstly, input multimedia signals including video, audio and data are coded by MPEG-2 (Moving Pictures Experts Group) [1] encoder.The generated MPEG-2 TS packets are multiplexed according to the TMCC (Transmission Multiplexing Configuration Control) sequence. TMCC represents the code rate, modulation format and segment assignment of the ISDB-T signal. Channel coding is performed after

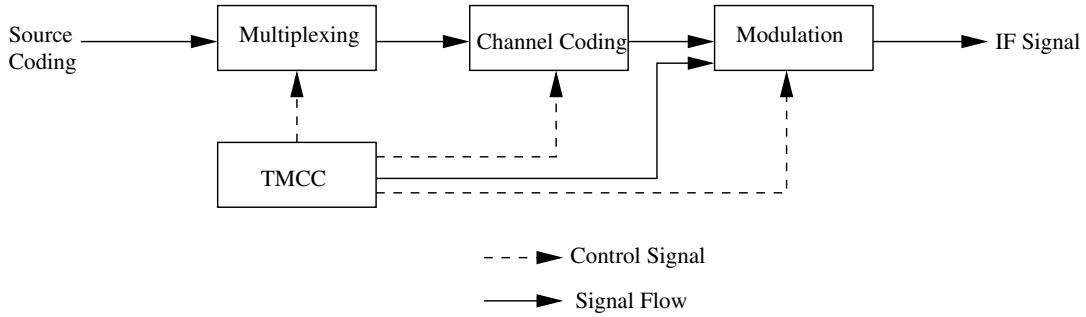

Figure 2.9. ISDB-T Transmitter Block Diagram

the multiplexing MPEG-e streams. As a channel coding RS (Reed-Solomon) code followed by the punctured convolutional code is employed. The code rate is controlled by TMCC sequence, as well as the multiplexing that. The channel coded transmitted signal is further multiplexed with TMCC signal and applied to the modulator. Modulation part does carrier modulation, whose modulation format is again controlled by TMCC sequence. Finally, IF(Intermediate Frequency) signals are outputted.

The emitted signal is described by the following expression:

$$s(t) \;=\; \mathbf{Re}\Big\{ e^{j2\pi f_c t} \sum_{n=0}^{\infty} \sum_{k=0}^{K-1} c(n,k)\Psi(n,k,t) \Big\} \tag{2.18}$$

where,

$$\Psi(n,k,t) = \begin{cases} e^{j2\pi \frac{k-K_c}{T_u}(t-T_g-nT_s)} & nT_s \le t < (n+1)T_s \\ 0 & t < nT_s, (n+1)T_s \le t \end{cases} \tag{2.19}$$

is the waveform of the $k-th$ sub-carrier at the $n-th$ OFDM symbol, where:

k : the carrier index numbered from 0^{th} carrier of the 11^{th};

n : the OFDM symbol number;

K : the number of transmitted carriers (Mode 1: 1405, Mode 2: 2809, Mode 3: 5617);

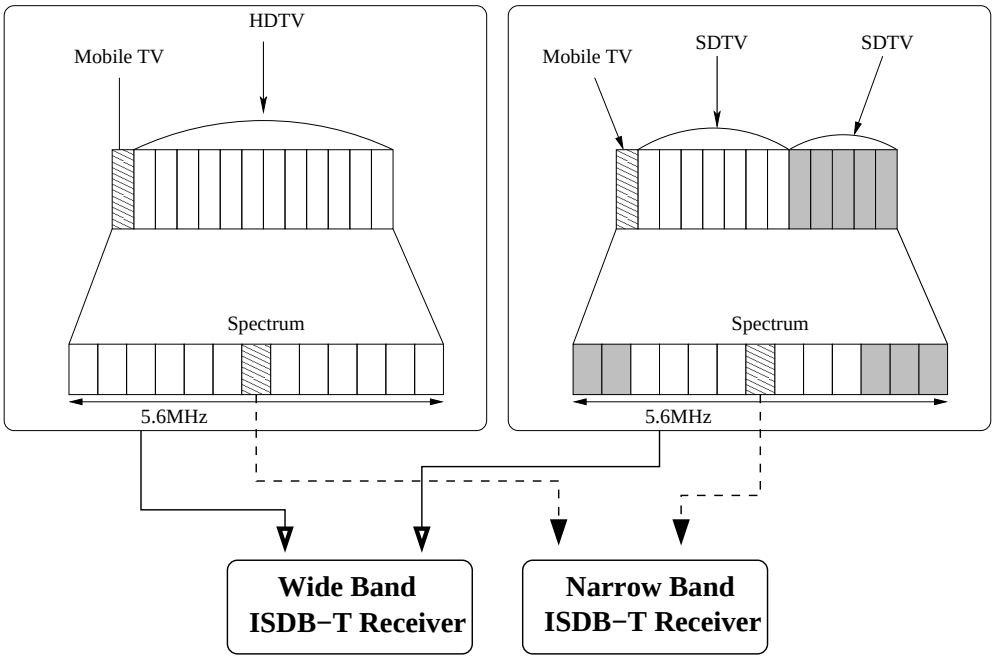

Figure 2.10. Hierarchical Transmission and Partial Reception

T_s : the symbol duration ($= T_g + T_u$);

T_g : the duration of the guard interval;

T_u : the duration of effective symbol;

f_c : the center carrier frequency of RF signal;

k_c : the carrier index of the center frequency of RF signal (Mode 1: $K_c = 702$, Mode 2: $K_c = 1404$, Mode 3: $K_c = 2808$);

$c(n, k)$: QAM symbol at the $n - th$ OFDM symbol corresponding to the $k - th$ sub-carrier;

$s(t)$: an RF signal.

Hierarchical Transmission

Hierarchical transmission of ISDB-T can be achieved by transmitting OFDM segment groups having different transmission parameters in a channel. As trans-

mission parameters of ISDB-T can be independently applied for each segment, for example, each segment has different modulation scheme of carriers, code rates of inner code and the length of the time interleaving. ISDB-T can be transmitted maximum of three layers in a channel at the same time.

Partial Reception

Partial reception contained in a transmission channel can be obtained a narrow-band receiver that has a bandwidth of one OFDM segment. It can be separated the segment independently from the neighbor segments. Because each OFDM segment has operated frequency interleaving independently the other OFDM segments. However, one segment for partial reception should be located central segment of OFDM segments. (See the Figure 2.10)

Table 2.1. Transmission Parameters for ISDB-T

Mode	Mode 1	Mode 2	Mode 3
Number of OFDM Segments	13		
Bandwidth	5.575 [MHz]	5.543 [MHz]	5.572 [MHz]
Carrier Spacing	3.968 [kHz]	1.984 [kHz]	0.992 [kHz]
Number of Carriers	1405	2809	5617
Number of Data Carriers	1248	2496	4992
Carrier Modulation	QPSK, 16QAM, 64QAM, DQPSK		
FFT Window Size	2048	4096	8192
FFT Sampling Speed	8.12698 [MHz]		
Effective Symbol Duration	252 [μs]	504 [μs]	1.008 [ms]
Guard Interval Ratio	1/4, 1/8, 1/16, 1/32		
Number of Symbol per Frame	204		
Error Correction(Inner Code)	Convolutional Code (Code Rate 1/2, 2/3, 3/4, 5/6, 7/8)		
Error Correction(Outer Code)	RS (204, 188)		

2.3.3 Transmission Parameters

Table 2.1 shows transmission parameters for ISDB-T. ISDB-T has three modes, namely, mode 1, mode 2 and 3, depending on the number of sub-carriers, while

Table 2.2. Information Rates(Mbit/s) of ISDB-T(13 Segments)

Carrier Modulation	Convolutional Code Rate	Guard Interval			
		1/4	1/8	1/16	1/32
QPSK	1/2	3.651	4.056	4.295	4.425
	2/3	4.868	5.409	5.727	5.900
DQPSK	3/4	5.476	6.085	6.443	6.638
	5/6	6.085	6.761	7.159	7.376
	7/8	6.389	7.099	7.517	7.744
	1/2	7.302	8.113	8.590	8.851
	2/3	9.736	10.818	11.454	11.801
16QAM	3/4	10.953	12.170	12.886	13.276
	5/6	12.170	13.522	14.318	17.752
	7/8	12.779	14.198	15.034	15.489
	1/2	10.953	12.170	12.886	13.276
	2/3	14.604	16.227	17.181	17.702
64QAM	3/4	16.430	18.255	19.329	19.915
	5/6	18.255	20.284	21.477	22.128
	7/8	19.168	21.298	22.551	23.234

its bandwidth is almost the same as 5.6MHz. In mode 1, there is 1404 sub-carriers whose frequency spacing is 4kHz. The symbol interval is 250μs. Mode 1 is sensitive to multi-path delay spread, because its effective symbol duration is short. However, it is robust to Doppler spread as high speed mobile reception and frequency offset, because its sub-carrier spacing is wide. In contrast to mode 1, mode 3 has 5617 carriers spaced in 1kHz in frequency. Mode 3 is robust to multi-path delay spread, because of long effective symbol duration. But, it is intolerance of Doppler spread as high speed mobile reception and frequency offset, because of small sub-carrier spacing.

For error correction, ISDB-T employs concatenated coding scheme. As an inner code, it employs punctured convolutional code. while Reed-Solomon (RS) (204, 188, 8) code is exploited as an outer code. The code rate and constraint length of the inner convolutional code are 1/2 and 7, respectively. The code rate is chosen from one of 1/2, 2/3, 3/4, 5/6, and 7/8 by selecting the puncturing pattern.

Broadcaster can select among three modes that they consider about propagation characteristic as multi-path delay. However, actually, mode 3 and 1/8 of guard interval ratio may be employed which has narrow sub-carrier spacing and good transmission efficiency. Also, it can be removed effect of multi-path delay.

Carrier modulation use 64QAM (Quadrature Amplitude Modulation) and QPSK (Quadrature Phase Shift Keying) which are digital modulation. In the case of stationary reception, which is more stability than mobile reception, use 64QAM and 7/8 or 3/4 of convolutional code rate. Therefore it could high speed transmission. Meanwhile, instability reception as mobile reception, employs QPSK and 1/2 or 2/3 of convolutional code rate because it needed error correction.

Table 2.2 represents information rates of ISDB-T. It provides various of information rates which are related guard interval ratio, carrier modulation scheme and convolutional code rates.

2.3.4 1 Segment Broadcasting

Table 2.3. ISDB-T 1 Segment Information Rates

Modulation Scheme	Code Rate	Information Rates
16QAM	1/2	624 kbps
QPSK	2/3	416 kbps
QPSK	1/2	312 kbps

Table 2.4. Details of ISDB-T 1 Segment Information Rates

	Information Rates
Video	128∼180 kbps
Audio	48∼64 kbps
Data	50∼60 kbps
Control signal, etc.	50 kbps
Total	312 kbps

ISDB-T 1 segment broadcasting service uses H.264/AVC (or H.264/MPEG-4 AVC) for its video and audio coding scheme. However, the original video coding

scheme was MPEG-4. Because of patent problem, H.264/AVC is to be video and audio coding scheme for ISDB-T 1 segment broadcasting service. So, 1 segment broadcasting service has delayed about 3 years.

Table 2.3 shows information rates of ISDB-T 1 segment according to the modulation scheme and code rate. QPSK can be supported more stable reception than 16QAM. However, 16QAM is provided high-speed transmission.

Table 2.4 shows details of ISDB-T 1 segment information rates. For stable mobile reception, ISDB-T 1 segment will employ QPSK modulation scheme and code rate is 1/2. Therefore, according to the Table 2.4, ISDB-T 1 segment needs 312 kbps of information rates.

2.4. DVB-T

2.4.1 Standard Overview

The European DTTB standard, DVB-T [3], was ratified in 1997 and the first commercial DVB-T broadcasts were performed by the United Kingdom in 1998. DVB-T based on OFDM for its transmission scheme and QPSK, 16QAM and 64QAM for its modulation scheme. Therefore, it is a flexible system allowing the broadcasters to select from a variety of options to suit their various service environments. DVB-T allows the broadcasters to match, and even improve on, the coverage of analog TV. Also, DVB-T can improve the efficiency of frequency usage to utilize SFN.

Figure 2.11 illustrates functional block diagram of DVB-T system. Firstly, the compressed video data, the compressed audio data and data streams are multiplexed into program streams. One or more program streams are combined into an MPEG-2 TS (Transport Stream), where its length is 188 bytes. The byte sequence of the MPEG-2 TS is scrambled by making use of energy dispersal. Next, the outer coder performs Reed-Solomon (RS) code, where its result data length is 204 bytes. The output data goes into the outer interleaver, which performs the convolutional interleaving. The interleaved data is encoded by a punctured convolutional code at the inner coder. The available code rate is 1/2, 2/3, 3/4, 5/6 and 7/8, respectively. Also, the inner interleaver rearranges the

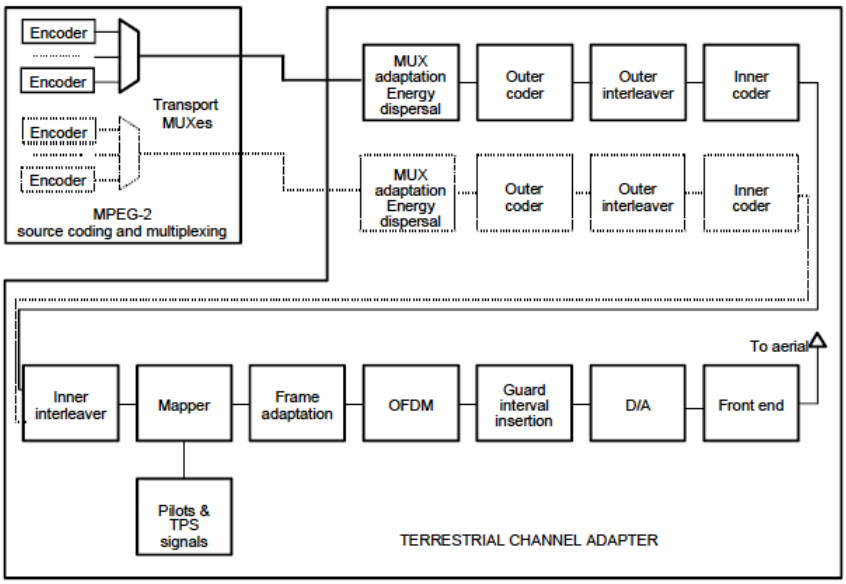

Figure 2.11. Functional Block Diagram of DVB-T System

data sequence, which is aiming to reduce the performance degradation due to burst error. Bit-wise interleaving and symbol interleaving are being used in the inner interleaver, both interleaving processes are block-based. The digital bit sequence is mapped into a base band modulated sequence of complex symbols. The valid modulation schemes are QPSK, 16QAM and 64QAM, respectively. The transmitted signal is organized in frames. Each frame has 68 OFDM symbols and each OFDM symbol is constituted by a set of 6817 sub-carriers in the 8K mode and 1705 sub-carriers in the 2K mode. In addition to the transmitted data, an OFDM frame contains scattered pilot (SP) carriers , continual pilot (CP) carriers and transmitter parameter signalling (TPS) carriers. The pilots can be used for frame synchronization, frequency synchronization, time synchronization, channel estimation, transmission mode identification. The transmitted signal is processed by FFT (Fast Fourier Transform) and inserted guard interval. Finally, the transmitted signal is transmitted via air. The emitted signal is similar to ISDB-T except for the number of sub-carriers.

According to Table 2.5, DVB-T has 8K mode and 2K mode, which are related FFT window size. The number of carriers is 6817 for 8K mode and 1705

Table 2.5. Transmission Parameters for DVB-T for 8 MHz channels

Mode	8K mode	2K mode
Number of Carriers	6817	1705
Bandwidth	7.61 [MHz]	7.61 [MHz]
Carrier Spacing	1.116 [kHz]	4.464 [kHz]
Carrier Modulation	QPSK, 16QAM, 64QAM	
FFT Window Size	8192	2048
Effective Symbol Duration	896 [μs]	224 [μs]
Guard Interval Ratio	1/4, 1/8, 1/16, 1/32	
Error Correction(Inner Code)	Convolutional Code (Code Rate 1/2, 2/3, 3/4, 5/6, 7/8)	
Error Correction(Outer Code)	RS (204, 188)	

Table 2.6. Useful bit rate (Mbit/s) for all combinations of guard interval, constellation and code rate for non-hierarchical systems for 8 MHz channels

Carrier Modulation	Code Rate	Guard Interval			
		1/4	1/8	1/16	1/32
QPSK	1/2	4.98	5.53	5.85	6.03
	2/3	6.64	7.37	7.81	8.04
	3/4	7.46	8.29	8.78	9.05
	5/6	8.29	9.22	9.76	10.05
	7/8	8.71	9.68	10.25	10.56
16QAM	1/2	9.95	11.06	11.71	12.06
	2/3	13.27	14.75	15.61	16.09
	3/4	14.93	16.59	17.56	18.10
	5/6	16.59	18.43	19.52	20.11
	7/8	17.42	19.35	20.49	21.11
64QAM	1/2	14.93	16.59	17.56	18.10
	2/3	19.91	22.12	23.42	24.13
	3/4	22.39	24.88	26.35	27.14
	5/6	24.88	27.65	29.27	30.16
	7/8	26.13	29.03	30.74	31.67

for 2K mode. The bandwidth is 7.61 MHz and the carrier spacings among subcarriers of 8K mode and 2K mode are 1.116 kHz and 4.464 kHz, respectively.

Table 2.6 shows useful bit rate for all combinations of guard interval, constellation and code rate for non-hierarchical systems for 8 MHz channels. The available bit rate is from 4.98 Mbit/s to 31.67 Mbit/s.

2.4.2 Hierarchical Modulation

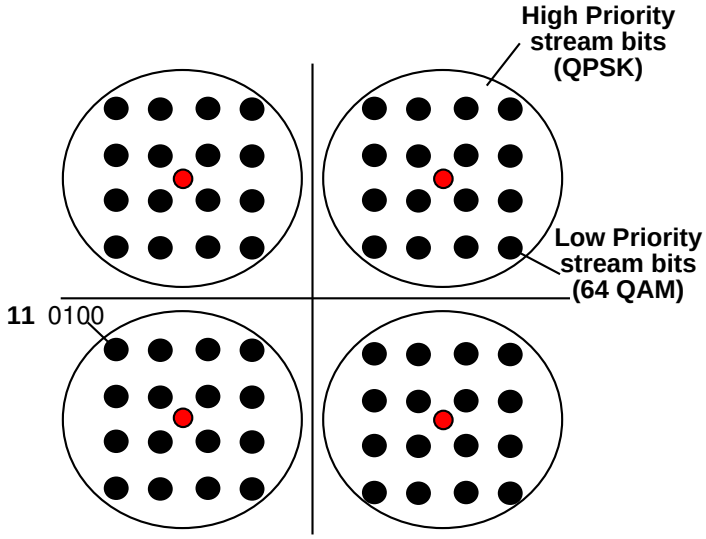

Figure 2.12. Hierarchical Modulation

The hierarchical modulation provides different error protection levels for two separate data streams in a single DVB-T stream. In ISDB-T, segment based hierarchical transmission is performed. In contrast, DVB-T employs non-uniform QAM for establishing hierarchical transmission. One stream, called the high priority (HP) stream is embedded within a low priority (LP) stream. Receivers can receive both streams if the reception condition is good. However, the reception condition is bad, receivers may only receive the HP stream. Broadcasters can provide two completely different services. Generally, the LP stream is capable of higher bit rate, but lower robustness against channel condition than HP one. Taking the example of 64QAM, the hierarchical system maps the data onto 64QAM in such a way that there is effectively a QPSK stream buried within 64QAM

stream. Furthermore, the spacing between constellation states can be adjusted to protect the QPSK (HP) stream, at the expense of the 64QAM (LP) stream. Figure 2.12 shows DVB-T hierarchical 64QAM constellation with an embedded QPSK stream.

Considering bits and bytes, in 64QAM can code 6 bits per 64QAM symbol. In hierarchical modulation, the 2 most significant bits (MSB) would be used for the robust mobile reception, while the remaining 6 bits would contain. See the Figure 2.12, the first MSBs, '11', correspond to the QPSK (HP) stream, for example, SDTV and the entire bits, '110100', correspond to the 64QAM (LP), for example, HDTV. Therefore, receivers can choose the each data stream in accordance with reception conditions or a specification of receiver.

2.5. T-DMB

2.5.1 Standard Overview

In South Korea, T-DMB service has started service on December 1, 2005. T-DMB service consists of 11 television channels, 25 radio channels and 3 data channels. In order to send multimedia data to mobile devices such as mobile phones and portable digital TV, T-DMB was standardized on July 2005. T-DMB uses VHF (Very High Frequency) band. T-DMB is especially based on Eureka 147 DAB (Digital Audio Broadcasting) [17] standard, employs transmission mode 1 out of DAB's 4 transmission modes. As illustrated in Figure 2.13, three T-DMB channels are allocated in one 6 MHz channel, which was used by the conventional analog TV channel.

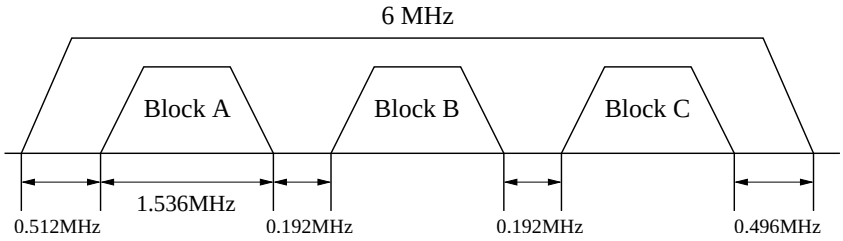

Figure 2.13. DMB Spectrum in VHF Band

2.5.2 Transmission System

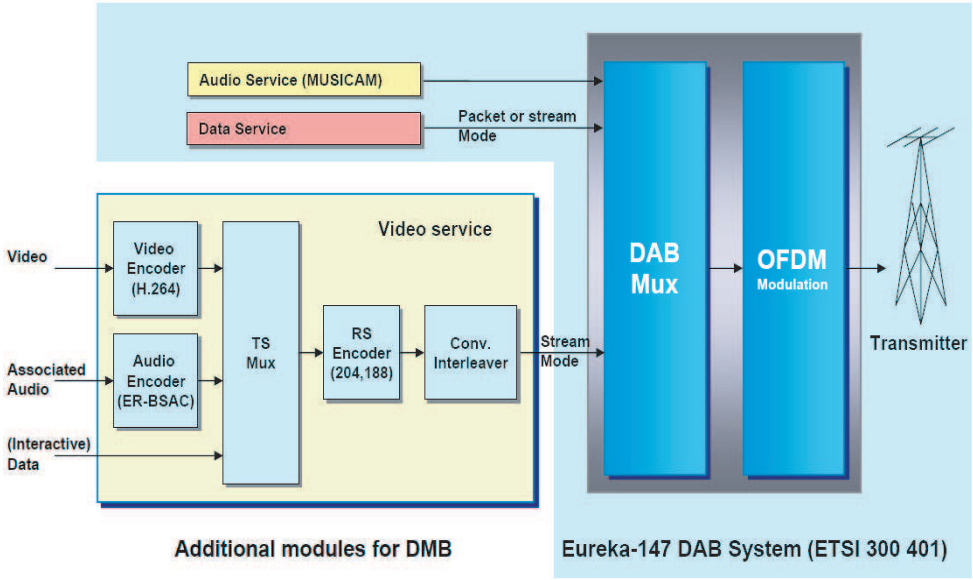

Figure 2.14. DMB System Structure

Figure 2.14 shows T-DMB system structure. In order to implement DMB system, it should be added video/audio encoder, RS (Reed-Solomon) encoder and convolutional interleaver. The encoded video, audio, and the auxiliary data information, which makes up a video service, are multiplexed into an MPEG-2 TS and further outer error correction is performed. MPEG-2 TS Modulation format of T-DMB is DQPSK (Differential encoded Quadrature Phase Shift Keying). DQPSK does not require any pilot symbols to estimate.

The phase reference since DQPSK represents the information by phase difference between consecutive two symbols, not by phase. Although the bit error rate (BER) performance of DQPSK is slightly worse than that of QPSK, DQPSK is robust to fast motion of the vehicle. Convolutional code rate and constraint length are used 1/4 and 7, respectively. Also, T-DMB can change convolutional code rate to employ RCPC (Rate Compatible Punctured Convolutional Code). Moreover, T-DMB employs UEP (Unequal Error Protection) and EEP (Equal Error Protection) for different application of convolutional code rate in accordance with a priority of service data structure. For example, in the case of audio

Table 2.7. TDMB Transmission Parameters

Parameter	
Bandwidth (MHz)	1.536
FFT Sizes	2 k, 1 k, 0.5 k, 0.25 k
Guard Intervals (us)	246, 123, 62, 31
Inner Modulation	DQPSK
Error Protection	Convolutional Code + RS FEC
Convolutional Code Rates	1/4, 3/8, 1/2, 3/4, 4/9, 4/7, 2/3, 4/5
Carrier Spacing	1kHz
Time Slicing	Micro Time Slicing
Protocol Stack	Raw MPEG-4 (No IP Layer)
Theoretical Data Rate (Mbps)	1.06 $\sim$ 2.3

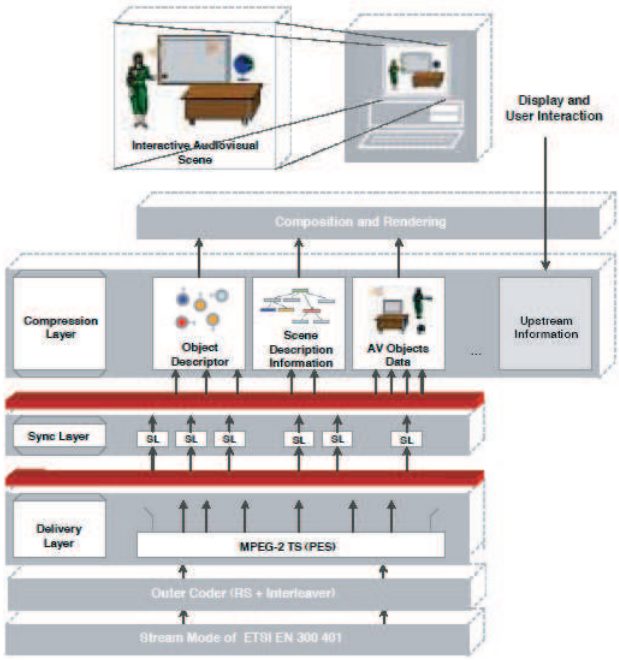

Figure 2.15. Conceptual Architecture for the Video Service

service, UEP is employed and in the case of data and video service, EEP is employed. Time interleaving is performed in 16 logic frames block (384ms) in order to disperse the error thanks to impulse noise. Furthermore, to mitigate channel deterioration due to frequency selective fading, frequency interleaving is performed. Effective symbol duration is 1ms and guard interval is 246 μs in order to prevent ISI (Inter Symbol Interference). The carrier spacing is 1kHz. Table 2.7 shows transmission parameters of T-DMB.

The video service is composed of three layers; content compression layer, synchronization layer, and transport layer. In the content compression layer, a specific video compression method is employed for the video contents, a specific compression method for the audio compression, and MPEG-4 BIFS (Binary Format for Scenes) for the auxiliary interactive data services. To synchronize the audio and video content, both temporally and spatially, MPEG-4 SL (Synchronization Layer) is employed in the synchronization layer. In the transport layer, MPEG-2 TS (Transport Stream) with some appropriate restriction is employed for the multiplexing of the compressed audio and video content. Figure 2.15 illustrates conceptual architecture for the video service.

2.5.3 Infrastructure

To provide T-DMB service, many base stations will be needed for expansion of reception area. Also, the broadcaster should be installed many repeaters such as subway stations and the inside of buildings, where does not reach the T-DMB signal.

In case of Korea, the cost for installation a base station and a repeater is huge. The broadcaster cannot make a benefit, if they only paid for installation a base station and a repeater. Therefore, the installation cost of base station and repeater shares with the beneficiaries, the broadcaster, mobile operator, and commodity provider.

Chapter 3

Impact of Doppler Spread on the BER Performance of OFDM System

3.1. Introduction

Although OFDM is robust to multi-path delay spreading as mentioned in Chapter 2, it is sensitive to ICI due to Doppler spread, since the frequency spacing between sub-carriers is narrow. By making use of AFC (Automatic Frequency Control) circuit, the frequency offset due to Doppler shift and inaccurate local oscillator at the receiver can be reduced. However, in multi-path environment, the received signal is composed of multiple paths with different Doppler shift frequency corresponding to its direction of arrival, or Doppler spread. AFC does not work when Doppler spread arises. Therefore, the performance of OFDM system is severely deteriorated by Doppler spread.

This chapter investigates impact of Doppler spread on the BER performance of OFDM system.

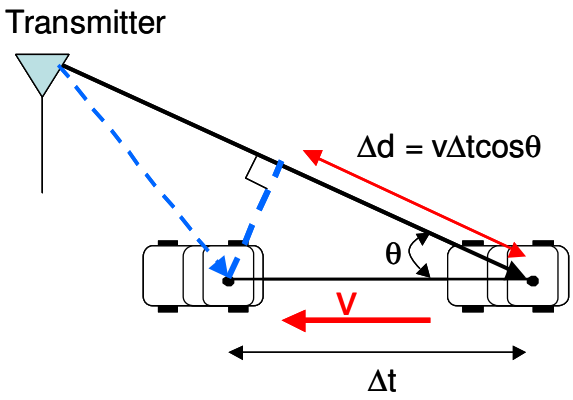

Figure 3.1. Geometry Associated with Doppler Shift

3.2. Doppler Spread

3.2.1 Doppler Shift for Single Incoming Wave

Now let's take a look at an overview of Doppler shift phenomenon. Assume that an incoming wave from the transmitter antenna comes from the direction as shown in Figure 3.1. The angle between the direction of incident wave and the direction of arrival of mobile traveling is defined as θ. The path length varies when the mobile receiver moves during a short time interval Δt. Due to the path length difference, the phase of transmitted signal is changed. Therefore, the Doppler shift frequency is obtained from the relationship between the carrier frequency and phase. The Doppler shift frequency is given by:

$$\begin{aligned} f_d &= \frac{1}{2\pi}\frac{\Delta\phi}{\Delta t} = v\cos\theta/\lambda \\ &= f_{dmax}\cdot\cos\theta, \end{aligned} \tag{3.1}$$

where

λ : the wavelength $(= \frac{c}{f_c})$;

f_c : the carrier frequency;

c : the speed of light$(= 3\times 10^8 m/s)$;

θ : the arrival angle of the received signal relative to the traveling direction of mobile;

Δd : a slight change in distance ($= v\Delta t\cos\theta$);

Δt : a short time interval;

$\Delta\phi$: the phase change in $\Delta t (= 2\pi v\Delta t\cos\theta/\lambda)$;

f_{dmax} : the maximum Doppler shift frequency ($= \frac{v}{\lambda}$).

3.2.2 Multi-Path Fading

In a practical mobile radio environment, there are a lot of propagation paths. The received RF signal exhibits extreme variations in both amplitude and phase. Multi-path fading is caused by multiple scattering of the waves due to the buildings and other structures nearby the mobile unit. However, it can be predicted by using powerful techniques of statistical communications theory.

Propagation Model

The envelope of the mobile radio signal is Rayleigh distributed when measured over distances of a few tens of wavelengths where the mean signal is sensibly constant [20]. This assumption that at any point the received field is made up of a number of horizontally traveling waves with random amplitudes and phases of arrival for different locations. Also, phases of the incoming waves are uniformly distributed from 0 to 2π. Besides, amplitudes and phases are assumed to be statistically independent. The received signal is given by

$$s(t) = E_0 \sum_{n=1}^{N} C_n \cos(2\pi f_c t + \theta_n) \tag{3.2}$$

where

$$\begin{aligned} \theta_n &= 2\pi f_n t + \phi_n, \\ f_n &= \frac{v}{\lambda}\cos\alpha_n \\ &= f_{dmax}\cos\alpha_n \end{aligned} \tag{3.3}$$

and f_c is the carrier frequency of the transmitted signal, E_0C_n is the amplitude of the nth incoming wave. The ϕ_n are random phase angles uniformly distributed from 0 to 2π. α_n denotes the angle of the nth incoming wave, f_n indicates a Doppler shift of the n th incoming wave.

The received signal, given by Equation 3.2, is assumed to be a Gaussian random processes due to application of central limit theorem. Equation 3.2 can be expressed in [21, 22]:

$$s(t) = T_c(t)cos\omega_c t - T_s(t)sin\omega_c t \tag{3.4}$$

where the in-phase (I) and quadrature-phase (Q) components of $s(t)$

$$T_c(t) = E_0 \sum_{n=1}^{N} C_n cos(\omega_n t + \phi_n), \tag{3.5}$$

and

$$T_s(t) = E_0 \sum_{n=1}^{N} C_n sin(\omega_n t + \phi_n) \tag{3.6}$$

are zero mean and statistically independent Gaussian random processes, respectively. The variance of the processes is given by

$$< T_c^2 >=< T_s^2 >=< |E_z|^2 >= \frac{E_0^2}{2} \tag{3.7}$$

where the random variables T_c and T_s are corresponding to $T_c(t)$ and $T_s(t)$ for fixed time t. The brackets indicate an ensemble average over the α_n, ϕ_n, and C_n.

The envelope and phase of the received signal $s(t)$ are respectively given by

$$r = \sqrt{T_c^2 + T_s^2}\theta = \tan^{-1}\frac{T_s}{T_c}$$

The probability density of r is Rayleigh distributed $p(r)$ as given by

$$p(r) = \begin{cases} \frac{r}{b}e^{-r^2/2b} & (r \geq 0) \\ 0 & (r < 0) \end{cases} \tag{3.8}$$

where $b = \frac{E_0^2}{2}$ is the mean power. On the other hand, the phase θ is uniformly distributed. The probability density function of θ is given by

$$p(\theta) = \begin{cases} \frac{1}{2\pi} & (0 \leq \theta < 2\pi) \\ 0 & (\text{otherwise}) \end{cases} \tag{3.9}$$

In this fading variation, the received signal is multiplexed with complex signal of random noise. In order to demodulate 64QAM or 16 QAM, which is a subcarrier modulation format of ISDB-T, the receiver has to compensate for the amplitude and phase variation due to fading.

Doppler Spread

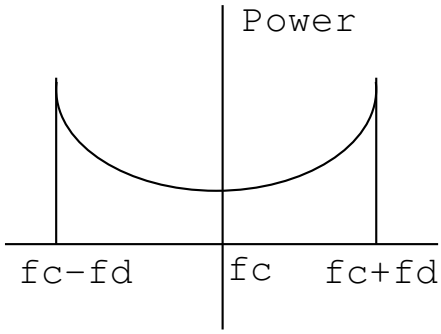

Figure 3.2. Doppler Power Spectral Density

In multi-path fading environment, the received signals, which are multiple scattering, are affected different Doppler shifts in accordance with its direction of arrivals. Thus, Doppler spread is caused by combining different Doppler shifts. In mobile communication system, the performance of receiver is deteriorated by Doppler spread which cannot reduce by making use of AFC.

As shown in Equation 3.3, the Doppler frequency shift is given by

$$f = f_{dmax}\cos\alpha \tag{3.10}$$

where α is uniformly distributed as shown in Equation 3.9. That is the received

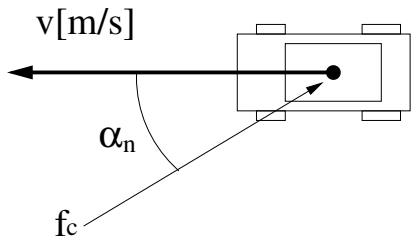

Figure 3.3. Moving Direction of Mobile and Direction of The Incident Wave

signal power incoming between α and $\alpha + d\alpha$ is given by

$$|\frac{b}{2\pi}d\alpha| = |S(f)df| \tag{3.11}$$

where $S(f)$ is the power spectral density. Since the derivative of Equation 3.10 is $df = -f_{dmax}\sin\alpha d\alpha$, Equation 3.11 becomes

$$S(f) = \frac{1}{\pi f_{dmax}\sqrt{1-(\frac{f}{f_{dmax}})^2}} \tag{3.12}$$

Figure 3.2 represents a Doppler power spectral density, $S(f)$, plotted as a function of Doppler-frequency shift. In the case of the omnidirectional antenna which has a uniform distribution of signals arriving at all arrival angles throughout the range (0, 2π) and is received an unmodulated continuous wave signal, the signal spectrum at the receive antenna terminal is given by [18, 19].

The range of frequency shift, f, is $f_c \pm f_d$. The Doppler power spectral would be zero outside the range of frequency shift. Equation 3.12 has been shown to match experimental data, which was gathered for mobile radio channel [20]. The largest magnitude of $S(f)$ occurs when the transmitted signal is received directly ahead of the moving antenna or directly behind it.

Coherence Time of the Channel

In the previous section power spectral density of the Doppler spreading channel is given by Equation 3.12. Fourier transformation of Equation 3.12

$$F\{S(f)\} = R(\tau) = bJ_0(2\pi f_{dmax}\tau), \tag{3.13}$$

is the auto-correlation function

In ISDB-T, the maximum Doppler shift frequency is f_{dmax}=107 [Hz], where its carrier frequency is f_c=770 [MHz], velocity, v, is 150[km/h]. In case of mode 3, 1/8 of the guard interval ratio, f_d=107 [Hz] gets to be done by

$$107[\text{Hz}]/1[\text{kHz}] = 0.107 \rightarrow 10.7\% \tag{3.14}$$

when the sub-carrier spacing is 1[kHz].

Delay Profile

In multi-path environment, each propagation path is not only different from other paths in the direction of arrival, but in the propagation path length. That is, the propagation delay is different from each other. This section describes the distribution of propagation delays which are used in this thesis.

The distribution of propagation delay is referred to as "delay profile". In the following, I employ three delay profiles, namely, equal gain two-ray delay profile, hilly terrain 6-tap and 12-tap models. The 6-tap and 12-tap delay profiles were modeled in GSM (Global System for Mobile Communications) standard.

Equal gain two-ray delay profile is shown in Table 3.1. Each tap has same average relative power and time difference is 4 μs. In this case, the transmitted signal is most severe interfered because the delayed transmitted signal has same average power as the transmitted signal, which does not delayed.

Table 3.1. Equal Gain Two-Ray Types

Tap No.	Relative Time(μs)	Average Relative Power(dB)
1	0	0
2	4	0

Table 3.2. GSM Hilly Terrain 6-Tap Types[26]

Tap No.	Relative Time(μs)	Average Relative Power(dB)
1	0	0
2	0.1	-1.5
3	0.3	-4.5
4	0.5	-7.5
5	15.0	-8.0
6	17.2	-17.7

Table 3.3. GSM Hilly Terrain 12-Tap Types[26]

Tap No.	Relative Time(μs)	Average Relative Power(dB)
1	0	-10
2	0.1	-8
3	0.3	-6
4	0.5	-4
5	0.7	0
6	1.0	0
7	1.3	-4
8	15.0	-8
9	15.2	-9
10	15.7	-10
11	17.2	-12
12	20.0	-14

Table 3.2 and 3.3 show the delay profiles of GSM hilly terrain 6-tap and 12-tap, respectively.

Chapter 4

Dipole Array Antenna Assisted Doppler Spread Compensator with MRC Diversity for ISDB-T Receiver

4.1. Introduction

This chapter proposes dipole array antenna assisted Doppler spread compensator with MRC diversity for ISDB-T receiver. Japanese DTTB standard, ISDB-T, employs OFDM for its transmission scheme. As I described in the previous chapter, OFDM is an efficient technique capable of high-speed digital transmission in a time-dispersive multi-path channel, because it has narrow bandwidth for all the sub-carriers. However, the performance of OFDM scheme can deteriorate by inter-channel interference (ICI), because OFDM has narrow frequency spacing among sub-carriers. ICI is caused by Doppler spread and carrier frequency offset (CFO) between a transmitter and a receiver. In ISDB-T, the frequency spacing among sub-carriers is about 1kHz. It means that ICI will degrade performance of OFDM system in the case of high-speed mobile reception.

The ICI due to CFO and Doppler shift may be solved by making use of automatic frequency control (AFC). However, in a multi-path environment, the

received signals are affected by a different Doppler shift, namely, Doppler spread, because the incoming waves arrive from different directions. In this case, AFC cannot remove the ICI.

To solve ICI due to Doppler spread, many researchers have proposed solution for reducing Doppler spread effect. In [7], the authors described CFO estimation based on frequency domain training sequence. According to this research, a transmitter needs training sequence for reducing frequency offset. However, in case of ISDB-T, the transmitter does not employ frequency domain training sequence. On the other hand, array antenna for reducing Doppler spread effect method has proposed [8]. In this method, the multi-path signals are separated according to their incident direction, with the result that the frequency shift of each beam signal is corrected. However, a number of array elements are needed and hardware complexity is increased in this method. Meanwhile, a simple Doppler compensation method has been proposed [9]. S.A. Husen and S. Baggen use Wiener filtering for utilizing the spectral and temporal correlation that exists between several OFDM symbols. Although it needs a single antenna, its signal processing part is more complex than our proposed scheme. In [23], T. Wada et al. introduced Doppler spread compensator, which uses array antenna, for compensating for the performance degradation of adaptive modulation scheme due to fast fading. This study did not consider the diversity reception in conjunction with the array antenna assisted Doppler spread compensator.

To mitigate performance degradation of ISDB-T receiver due to Doppler spread, a linear array antenna assisted Doppler spread compensator has been proposed by Okada et al [10]. It estimates the received signal at a fixed point with respect to the ground by making use of the received signals from several array elements followed by a space domain interpolator. The authors showed that it can mitigate the deterioration in BER performance due to Doppler spread.

Although, the conventional Doppler spread compensator is an efficient anti-Doppler spread compensation technique, it has a drawback in terms of the mutual coupling effect between array elements. As pointed out in the reference [10], the mutual coupling degrades the performance of the Doppler spread compensator.

Polarization mismatching between the transmitter and the receiver is another problem in efficient reception of DTTB signals. In Japan, almost all DTTB

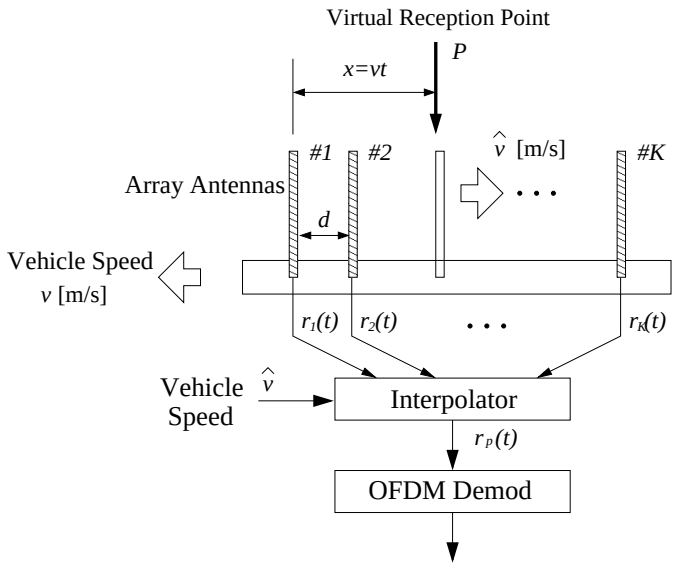

Figure 4.1. Block diagram of the conventional Doppler spread compensator

stations transmit their signals in horizontal polarization. This implies that efficient reception of DTTB signals requires a horizontally-polarized antenna. However, the conventional scheme employs a vertical-polarization monopole array. This polarization mismatching reduces the received signal strength. Furthermore, due to fading, OFDM itself cannot be a solution for degradation.

To solve these problems, I propose a dipole array antenna assisted Doppler spread compensator with maximum ratio combining (MRC) diversity receiver. In antenna simulation, I assumed the mutual coupling effect between each array element. Besides, to make use of MRC diversity, the BER performance has been improved in a multi-path fading channel.

4.2. System Model

4.2.1 The Conventional Doppler Spread Compensator

Figure 4.1 shows the structure of the conventional Doppler spread compensator, which was first proposed in [10] and [24]. The K-elements of monopole antennas are lined up on top of the vehicle as in Figure 4.1. The array elements are aligned

parallel to the direction of motion of the vehicle. The spacing between elements is d(m). Signals received at the corresponding array elements are applied to the space domain interpolator, which estimates the received signal at a stationary point with respect to the ground.

Let us assume that the vehicle travels at a velocity of v(m/s), and the DTTB receiver knows its velocity. This assumption is reasonable, because almost all vehicles have speedometers for measuring their velocities.

The space domain interpolator estimates the received signal at the virtual reception point P, which is $x = vt$ apart from the first array element. Since the reception point P does not move with respect to the ground, the received signal does not affect the Doppler phenomenon. That is, the performance degradation due to Doppler spread can be compensated by the proposed scheme.

4.2.2 Dipole Array Assisted Doppler Spread Compensator

Although the conventional Doppler spread compensator described in Sec. 4.2.1 is efficient, it has three problems, as follows.

1. Mutual Coupling: Since the spacing between elements is small, the mutual coupling effect is large and it degrades the compensation performance.

2. Polarization mismatch between transmitter and receiver antennas: The proposed scheme employs a vertically polarized monopole antenna, while the ISDB-T broadcasting station emits horizontally polarized signals.

3. Anti-fading: The conventional system does not have a diversity reception capability, even though it has multiple elements.

To solve these problems, I propose a new array antenna assisted Doppler spread compensator as shown in Figures 4.2 and 4.3. Simulation model is explained in Sect.4.3.

The polarization mismatch loss between a vertically polarized antenna and a horizontal polarized antenna is an infinite quantity, theoretically. Also, the experimental value of the polarization mismatch loss is up to 20dB which value is given by [27]. In this paper, I do not describe about polarization mismatch loss.

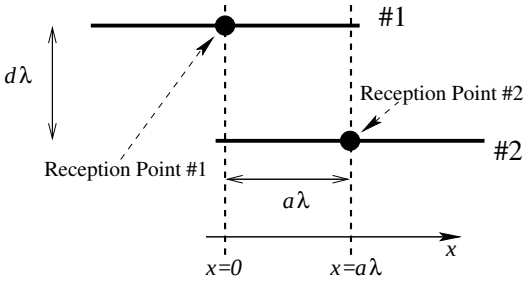

(a) Configuration of the Proposed Dipole Array

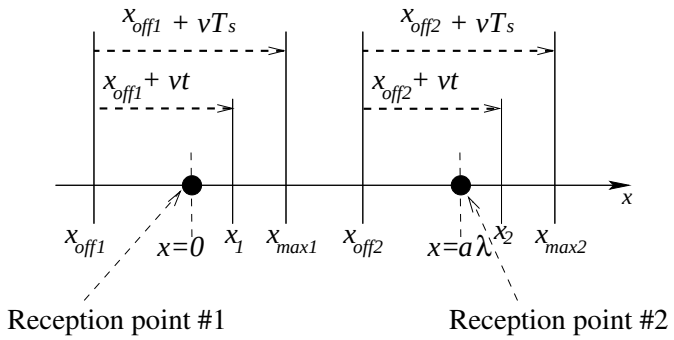

(b) Reception points Estimated by the Interpolator

Figure 4.2. Configuration and Reception Point of the Proposed Dipole Array(T_s: OFDM Symbol Time)

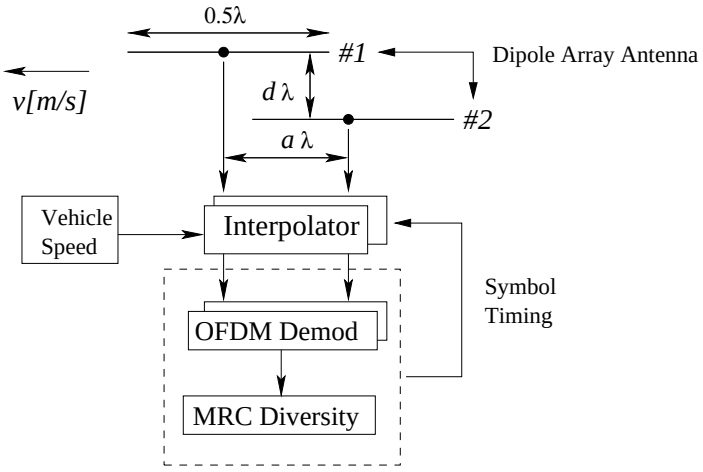

Figure 4.3. Block diagram of the proposed system

Figures 4.2 and 4.3 illustrate the proposed system, which is composed of dipole array elements and a space domain interpolator, the MRC diversity. The array elements are spaced vertically; $d\lambda$ and $a\lambda$ are the spacing between reception points, where λ is the wavelength of the carrier frequency signal. The received signals are applied to two space domain interpolators to estimate two different points,

$$x_1 = vt + x_{off1} \quad (x_{off1} = -vT_s/2) \tag{4.1}$$

and

$$x_2 = vt + x_{off2} \quad (x_{off2} = a\lambda - vT_s/2), \tag{4.2}$$

where T_s indicates the OFDM symbol interval. The reason why I set the x_{off1} and x_{off2} is given in Appendix B.

The received signal $\mathbf{r}(t) = [r_1(t), r_2(t)]^T$ is applied to the space domain interpolator to estimate the received signal at position x,

$$\tilde{r}(x,t) \;=\; \mathbf{w}^H(x)\mathbf{r}(t), \tag{4.3}$$

where $\mathbf{w}(x)$ is a weight vector. The derivation of the weight vector is given in Appendix A.

The output signals of the space domain interpolator are subjected to demodulation, and MRC diversity is then performed.

The position of virtual reception point resets each OFDM symbol as illustrated Figure 4.3.

Figure 4.4 shows the position of each reception point x_1 and x_2, which is fixed with respect to the ground during OFDM symbol duration. Therefore, space domain interpolator can compensate performance degradation due to Doppler spread.

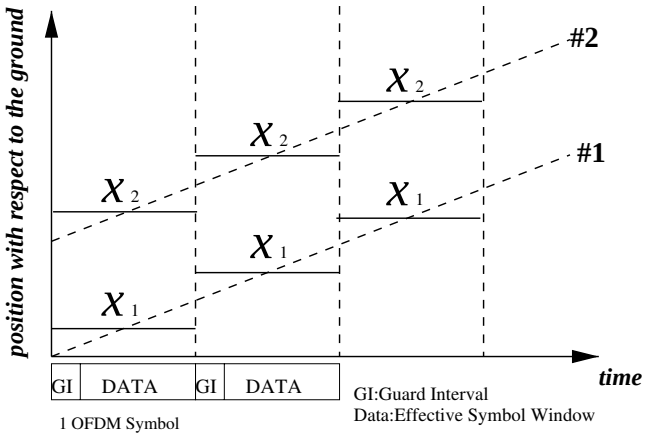

Figure 4.4. The receiving point to be estimated by the interpolator

4.3. Numerical Results

4.3.1 Simulation Parameters

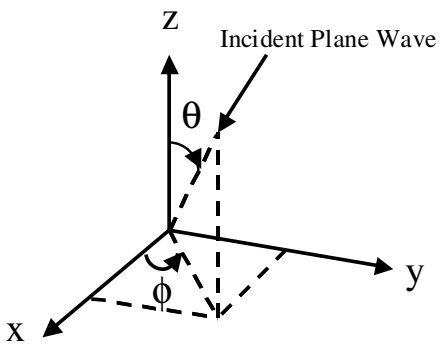

Figure 4.5. θ and ϕ

To evaluate the performance of the proposed system, I carried out a computer simulation. First, to use the phase and amplitude of each array element according to the direction of the arriving signal, the antenna simulation was implemented by making use of NEC-2(Numerical Electromagnetic Code-2), which analyzes the antenna using the moment method [25]. Incident plane wave is ra-

Table 4.1. Antenna Simulation Parameters

Frequency	500MHz
Load Impedance	50Ω
Source	Incident Plane Wave ($\theta = 70^\circ \sim 110^\circ$, $\phi = 0^\circ \sim 360^\circ$)
Antenna Length	0.5λ

Table 4.2. System Configuration

Transmission Parameters	
Bandwidth	5.572 MHz
Carrier Spacing	0.992 kHz
FFT size	8192
Number of Carriers	5617
Number of Data Carriers	4992
Carrier Modulation	64 QAM
Effective Symbol Duration	1.008ms
Guard Interval	126μs(1/8)
Propagation Model	
Model	Equal gain two-ray Rayleigh fading, GSM Model (Hilly terrain 6-ray and 12-ray)
Direction of Arrival	Uniform distribution

diated from outside to the array antenna. The received signals affected mutual coupling in accordance with antenna spacing. Table 4.1 shows the array antenna simulation parameters. As shown in Figure 4.5, θ and ϕ are expressed an angle between z and $x-y$ plane and an angle between x axis and y axis, respectively.

Next, the phase and amplitude values, which arrive from several directions randomly, are used in the computer simulation according to the ISDB-T standard. These phase and amplitude values used to make the received signal by multiplying the transmitted signal, which is also multiplied by fading channel information. The ISDB-T transmission parameters are shown in Table 4.2 [4]. I also assumed two types of propagation model. One is equal gain two-ray Rayleigh fading, where the delay time between each ray is 4μs, by Jakes' method [20]. The other is a typical hilly-terrain model given by the GSM (Global System for Mobile communications) standard [26].

4.3.2 Optimization According to Antenna Spacing

In this section, I derive the optimum antenna spacing in both the monopole array and the dipole array, when E_b/N_0 is 20dB and the normalized maximum Doppler frequency f_dT_s is 0.1.

The BER performance of the monopole array with a large mutual coupling effect and with various antenna spacings, d, was examined. According to Figure 4.6(a), the optimum antenna spacing, d, is $0.25[\lambda]$.

In the case of the dipole array, optimum antenna spacing, d, the spacing between reception point, a, and the BER performance is given in Figure 4.6(b). The optimum antenna spacing, d, and the optimum spacing between reception points, a, is $0.325[\lambda]$ and $0.2[\lambda]$, respectively.

Doppler spread compensator uses correlation value of each received signal from #1 and #2 elements. Correlation value is changing due to antenna spacing. Furthermore, the estimation range is set in proportion to vehicle speed. Therefore, BER performance varies depending on the antenna spacing as shown in Figure 4.6.

In the following, the optimum a and d are assumed to evaluate the efficiency of the proposed scheme in a mobile environment.

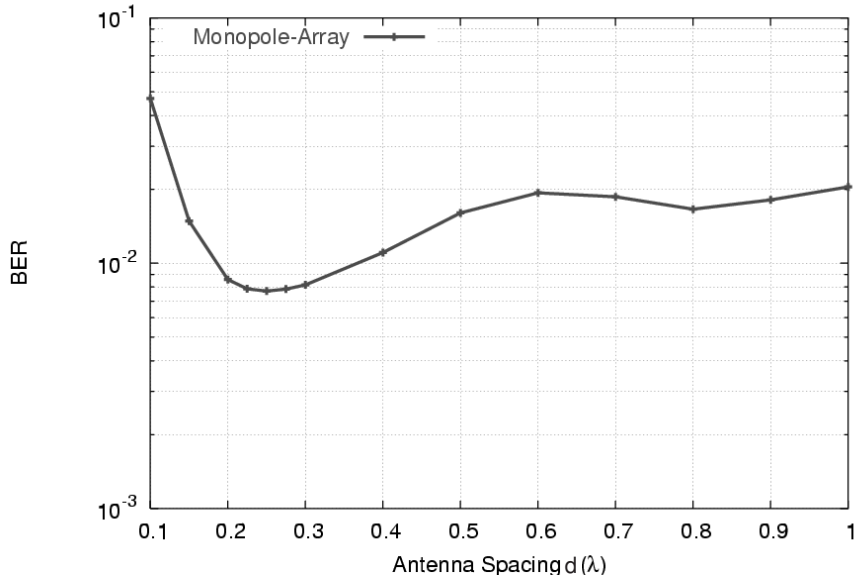

(a) Monopole Array

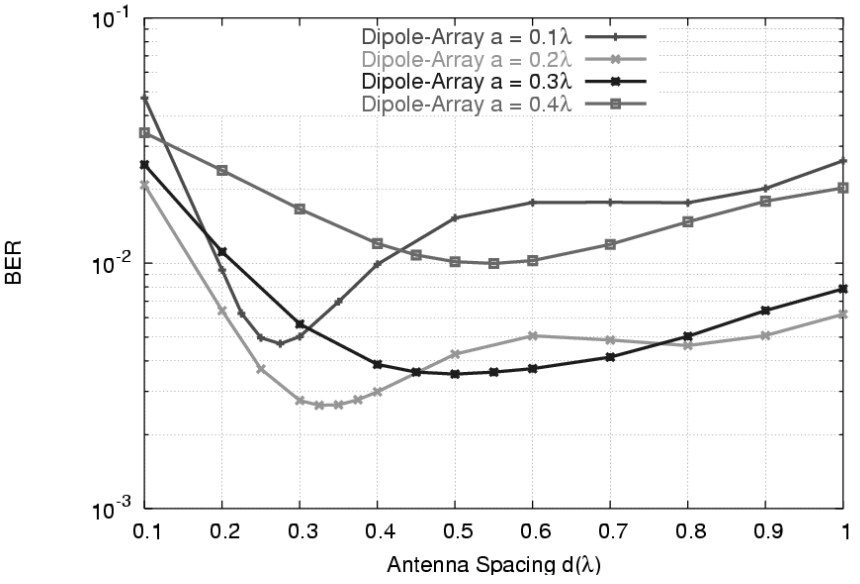

(b) Dipole Array

Figure 4.6. BER performance against Antenna Spacing when $E_b/N_0 = 20$dB and $f_d T_s = 0.1$

4.3.3 BER performance of the Monopole Array

In this section, I analyze the BER performance of the monopole array assisted Doppler spread compensator with MRC diversity receiver by computer simulation.

Figures 4.7(a) and 4.7(b) show the BER performance of various monopole-array receivers against $f_d T_s$ and E_b/N_0, respectively, when the optimum antenna spacing, d, is $0.25[\lambda]$ in a two-ray Rayleigh fading channel. The receiver using only MRC diversity has better BER performance than the receiver using only the Doppler spread compensator. Moreover, the proposed scheme has better BER performance than the others.

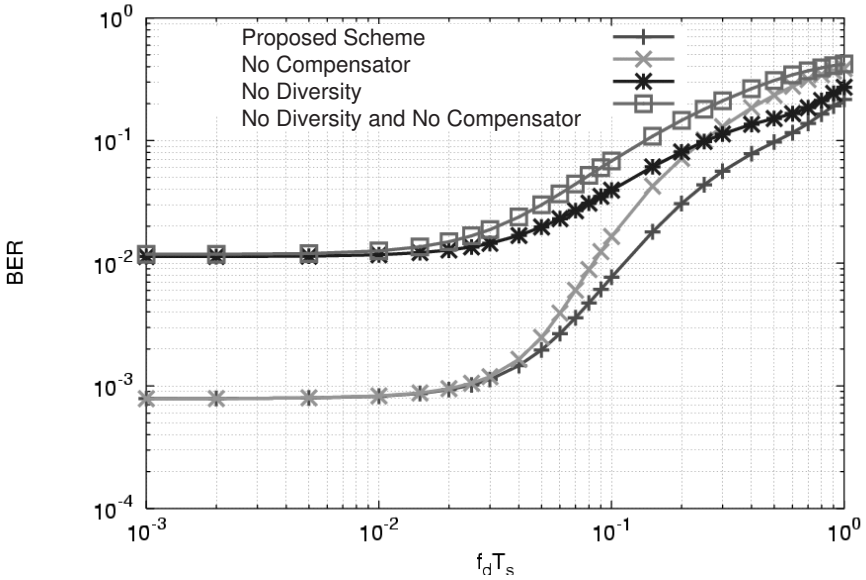

(a) BER performance of Monopole Array against f_dT_s ($E_b/N_0 = 20$dB)

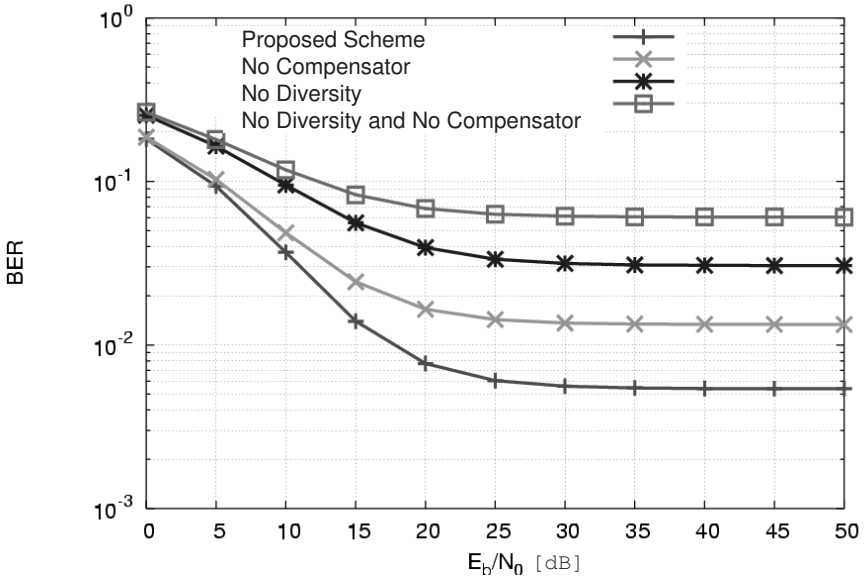

(b) BER performance of Monopole Array against E_b/N_0 ($f_dT_s = 0.1$)

Figure 4.7. BER performance of Monopole Array ($d = 0.25\lambda$)

4.3.4 BER performance of the Dipole Array

Figure 4.8(a) shows the BER performance of the various dipole-array receivers against f_dT_s, when E_b/N_0 is 20dB and when the antenna spacing, d, and the spacing between reception points, a, are 0.325λ and 0.2λ, respectively. In the low normalized maximum Doppler frequency region, the receiver with diversity function only gives better BER performance than the receiver with Doppler spread compensator only. However, when the normalized maximum Doppler frequency f_dT_s is more than 0.08, the receiver with Doppler spread compensator only outperforms the receiver with diversity function only. On the other hand, both receivers give better BER performance than a receiver without the Doppler spread compensator and diversity function. Figure 4.8(b) shows the BER performance of the various receivers against the E_b/N_0 when f_dT_s is 0.1 and the antenna spacing, d, and the spacing between reception points, a, are 0.325λ and 0.2λ, respectively.

According to Figures 4.8(a) and 4.8(b), the proposed scheme is the better in terms of BER performance than the others.

The diversity gain and the performance of Doppler spread compensator is trade-off because if the antenna spacing is narrow, and Doppler spread compensator improves its performance but if the antenna spacing is wide, diversity gain is increased. According to the optimization result, I find adequate antenna spacing for both Doppler spread compensator and diversity. Also, Figure 4.7(a) and Figure 4.8(a) shows the proposed scheme, which has MRC diversity function and Doppler spread compensator. From Figure 4.7(a) and Figure 4.8(a), the proposed scheme shows the best BER performance than the others.

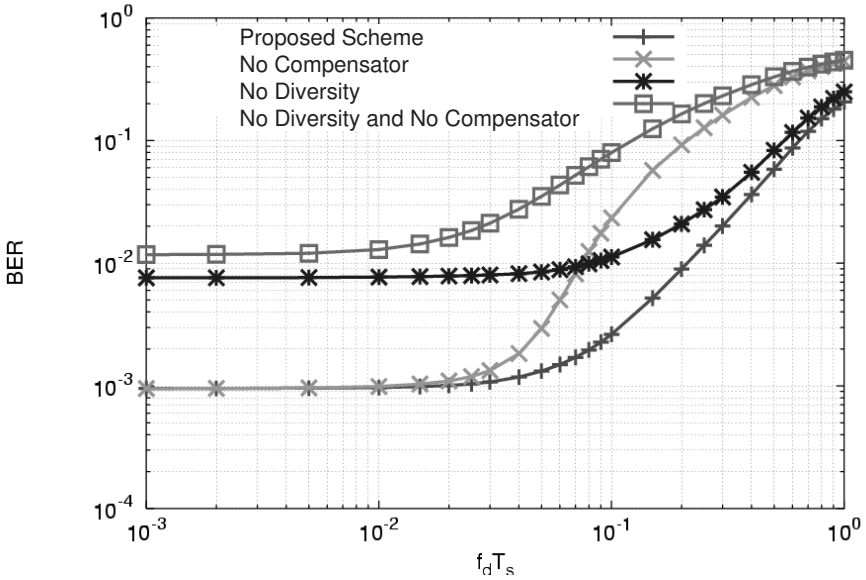

(a) BER performance of Monopole Array against f_dT_s ($E_b/N_0 = 20$dB)

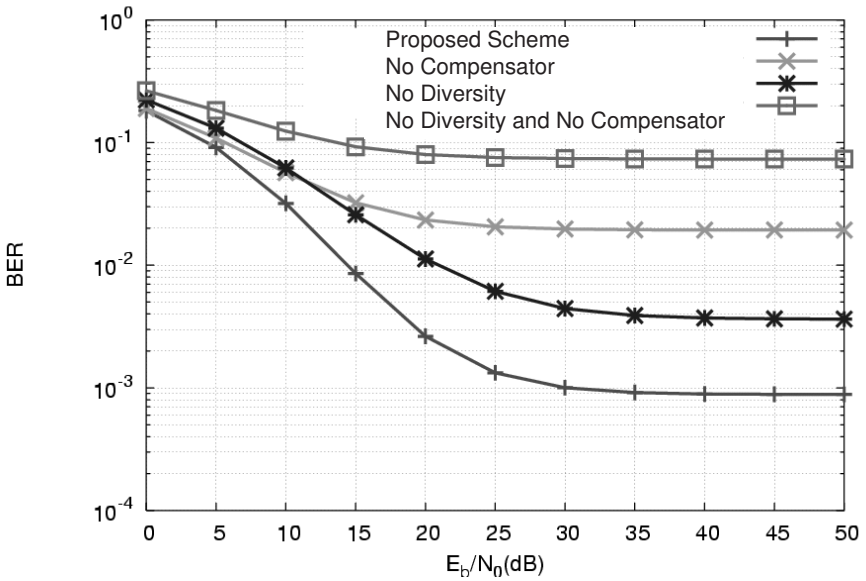

(b) BER performance of Dipole Array against E_b/N_0 ($f_dT_s = 0.1$)

Figure 4.8. BER performance of Dipole Array ($d = 0.325\lambda$, $a = 0.2\lambda$)

4.3.5 Consideration of the Elevation Angle Effect of Incident Wave

In this section, I consider the elevation angle effect of the incident wave.

The BER performance of the monopole array, which is a vertically polarized antenna, against the standard deviation of elevation angle of the incident wave is shown in Figures 4.9(a) and 4.9(b). It can be seen that the BER performance of the monopole array receiver does not deteriorate despite the elevation angle effect of the incident wave. This is because all the antenna elements are placed at the same height.

Also, according to Figures 4.10(a) and 4.10(b), the BER performance degradation due to the elevation angle effect is not particularly deteriorate incident wave, when the standard deviation, σ, is 0 to 5. However, the degradation becomes large when the value of σ is 10. In spite of the elevation angle effect of the incident wave, the dipole array receiver has a better BER performance than the monopole array receiver.

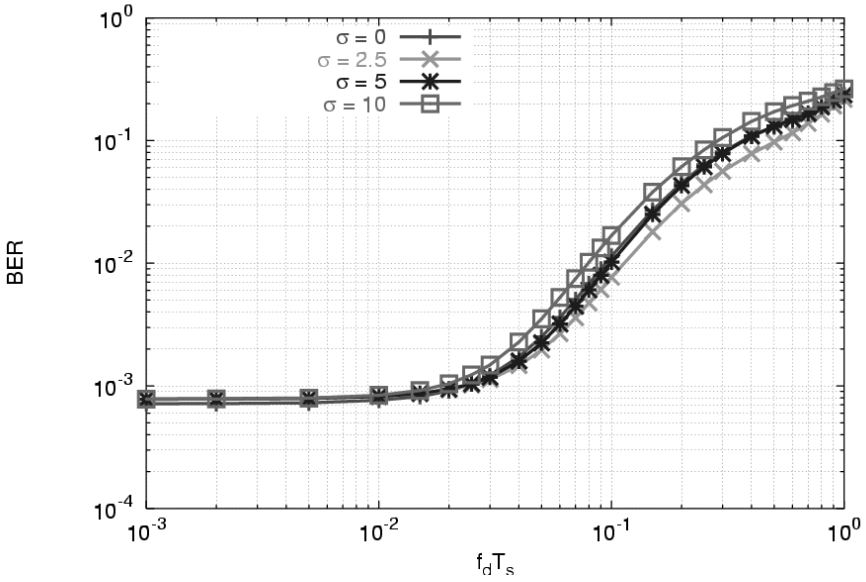

(a) BER performance of Monopole Array according to the elevation angle and f_dT_s ($E_b/N_0 = 20$dB)

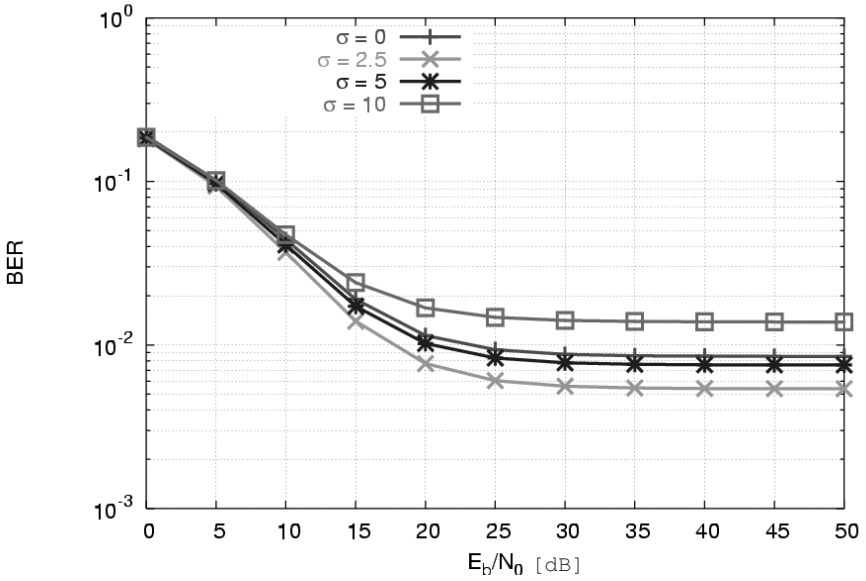

(b) BER performance of Monopole Array according to the elevation angle and E_b/N_0 ($f_dT_s = 0.1$)

Figure 4.9. BER performance of Monopole Array according to the elevation angle ($d = 0.25\lambda$

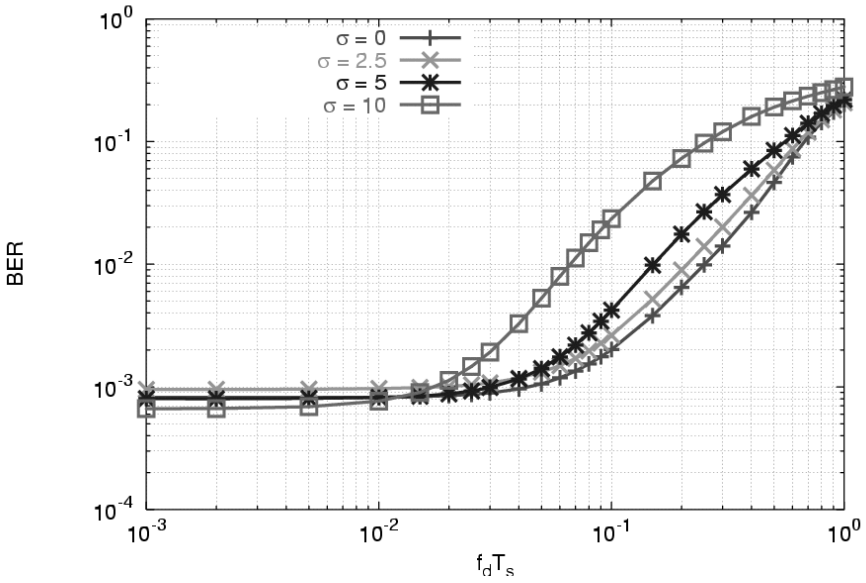

(a) BER performance of Monopole Array according to the elevation angle and f_dT_s ($E_b/N_0 = 20$dB)

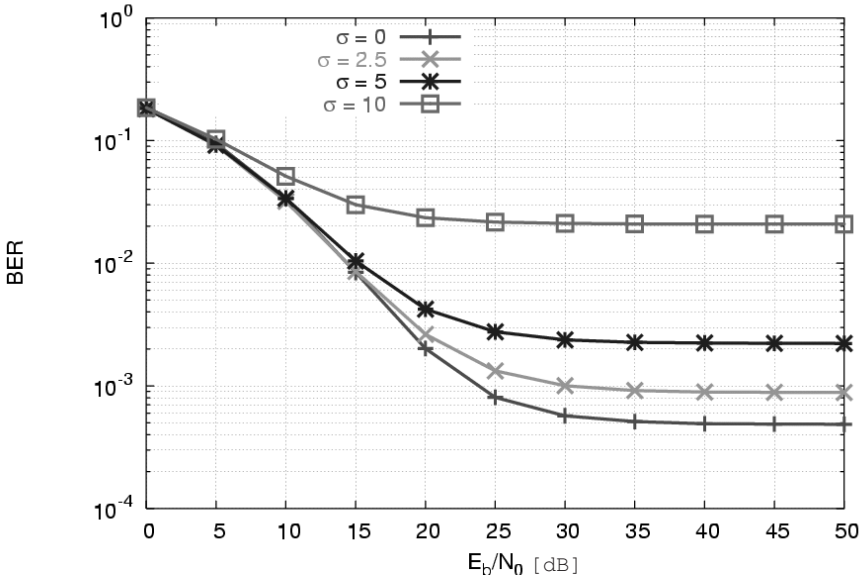

(b) BER performance of Monopole Array according to the elevation angle and E_b/N_0 ($f_dT_s = 0.1$)

Figure 4.10. BER performance of Dipole Array according to the elevation angle ($d = 0.325\lambda$, $a = 0.2\lambda$)

4.3.6 BER performance According to the Propagation Model

To evaluate the proposed scheme in various propagation models, I analyzed the BER performance by making use of the two-ray Rayleigh fading model [20] and GSM hilly terrain fading models[26].

Figures 4.11(a) and 4.11(b) show the BER performance of the proposed dipole array receiver against $f_d T_s$ and E_b/N_0 in the various propagation models. The average relative power of the two-ray Rayleigh fading model is 0dB. According to Figures 4.11(a) and 4.11(b), the proposed dipole array receiver, which has assisted the Doppler spread compensator with MRC diversity function, has good BER performance in the various propagation models tested.

There is no delay path exceeding guard interval in the propagation models I have simulated. Furthermore, I only evaluated the performance without forward error correction coding. Therefore, the BER performance is independent of delay profile as seen in Figure 4.11(a)and 4.11(b).

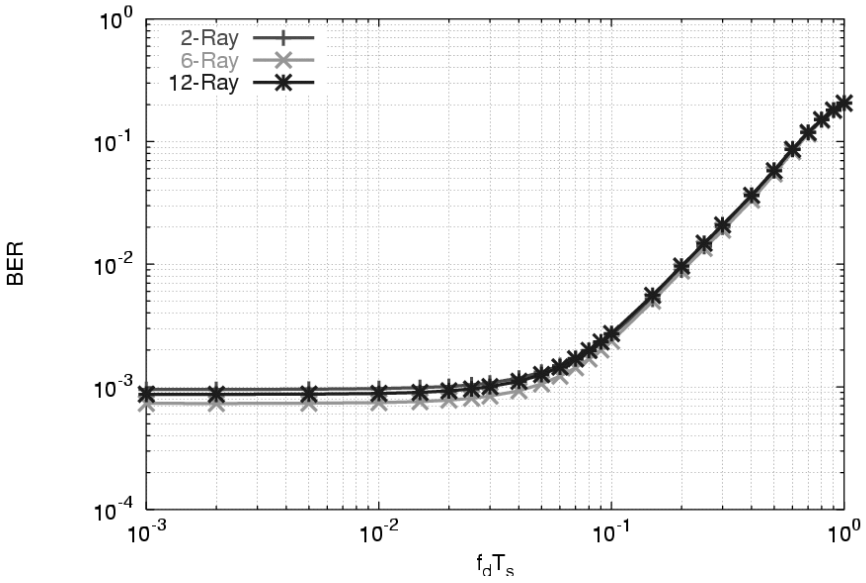

(a) BER performance of Dipole Array according to the Propagation Model and f_dT_s ($E_b/N_0 = 20$dB)

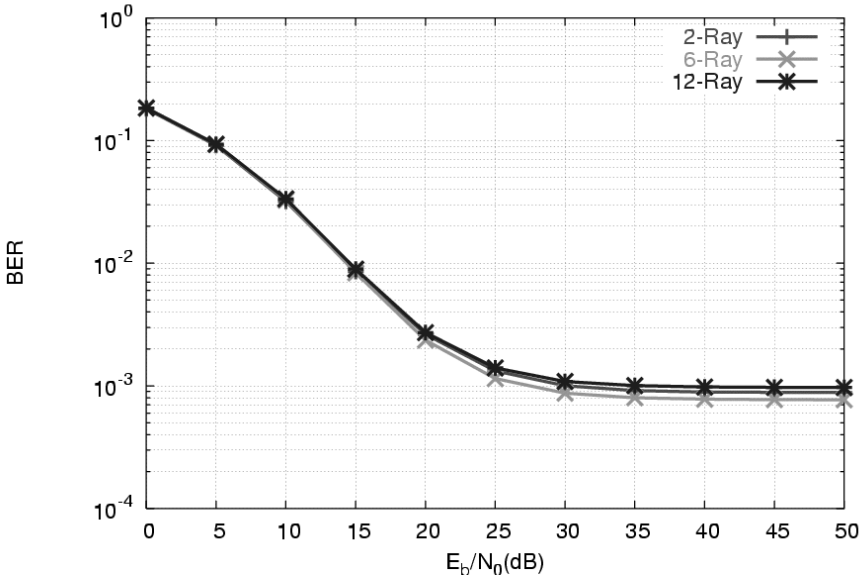

(b) BER performance of Dipole Array according to the Propagation Model and E_b/N_0 ($f_dT_s = 0.1$)

Figure 4.11. BER performance of Dipole Array according to the Propagation Model ($d = 0.325\lambda$, $a = 0.25\lambda$)

4.4. Conclusion

In this chapter, I have proposed array antenna assisted Doppler spread compensator with MRC diversity for a mobile DTTB receiver. The optimum antenna spacing and spacing between reception points were determined by computer simulation. The optimum antenna spacing of the monopole array is $0.25[\lambda]$, while the optimum antenna spacing and the spacing between reception points of the dipole array are $0.325[\lambda]$ and $0.2[\lambda]$, respectively. I then have analyzed the BER performance of the proposed monopole array receiver and dipole array receiver by making use of the optimum antenna spacing and the spacing between reception points. According to the computer simulation results, the proposed dipole array receiver has better BER performance than the monopole array receiver. Furthermore, to verify the validity of the proposed scheme, I analyzed how the BER performance of the proposed scheme was affected by the elevation angle of the incident wave. The vertically polarized monopole array receiver was not particularly affected by the elevation angle of the incident wave. However, the horizontally polarized dipole array receiver showed deterioration in BER performance when the standard deviation, σ, of the elevation angle was 10; however, it did not show high deterioration when the standard deviation was 0 to 5. The proposed dipole array receiver, which had better BER performance than the monopole array receiver, also had good BER performance regardless of the various propagation models.

Chapter 5

Effect of Dummy elements on a Monopole Array-assisted Doppler Spread Compensator for a Digital Terrestrial Television Broadcasting Receiver

5.1. Introduction

Recently, digital terrestrial television broadcasting (DTTB) has begun in many parts of the world. Among them, the European digital video broadcasting for terrestrial (DVB-T) [3] and the Japanese integrated services digital broadcasting for terrestrial (ISDB-T) [4] employ orthogonal frequency multiplexing division (OFDM) for their transmission schemes, and the Korean digital multimedia broadcasting (DMB) [5] also employs OFDM. OFDM is capable of high-speed digital transmission in a time-dispersive multi-path channel, and is also robust against frequency selective fading by multi-path delay spreading because of narrow bandwidth between the sub-carriers. Therefore, its hardware complexity is significantly reduced in comparison to a single carrier system with a time-domain equalizer [15]. The OFDM system is also capable of single-frequency networks

(SFN), which is especially effective in improving frequency utilization efficiency of a national DTTB network.

On the other hand, due to the narrow bandwidth between the sub-carriers, OFDM is sensitive to inter-channel interference (ICI). ICI is caused by Doppler spread, where several incoming waves affect the different Doppler shift, as well as by frequency offset between the transmitter and receiver.

In this chapter, I consider mode 3 of the Japanese DTTB system ISDB-T, which has 5617 sub-carriers and 1kHz of frequency spacing among sub-carriers. The maximum Doppler shift frequency reaches 70Hz when the carrier frequency is 770MHz and the receiver moves at 100km/h. This implies that the bit error rate (BER) performance is severely degraded by the Doppler spread effect.

To solve this problem, a linear array antenna-assisted Doppler spread compensator has been proposed by Okada et al. [10, 24, 11]. The proposed Doppler spread compensator was composed of a linear array antenna and a space domain interpolator. The space domain interpolator estimates the received signals at a fixed position with respect to the ground by using the received signals from each array element. Consequently, it could reduce BER performance degradation caused by the Doppler spread effect.

However, the mutual coupling effect changes the radiation patterns of each array element. The space domain interpolator is difficult to estimate the received signals at a fixed position with respect to the ground because the radiation patterns from each array element are different. Therefore, the performance of a Doppler spread compensator deteriorates due to the mutual coupling effect.

To reduce the mutual coupling effect, the proposed Doppler spread compensator has employed a mutual coupling canceller [10, 11], which calculates a mutual impedance matrix normalized by the load impedance. Hence, the mutual coupling canceller is sensitive to changes of carrier frequency. Moreover, its operating bandwidth is narrow compared with the television frequency band [10, 11]. For reference, the carrier frequency of ISDB-T is from 470MHz to 770MHz, and its bandwidth is 300MHz.

The use of dummy elements for reducing mutual coupling effect is already proposed[12, 13]. In [12], dummy elements are terminated with matched loads on each side of array to provide a similar environment for all the inner array elements.

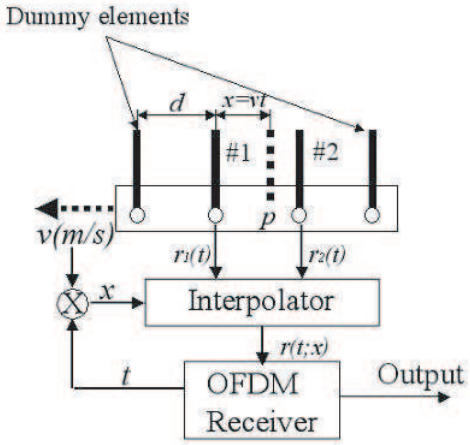

Figure 5.1. Block diagram of the Proposed Doppler Spread Compensator

This method is a simple way to reduce mutual coupling effect. However, it needs more space to set the arrays and more elements.

In this chapter, I use dummy elements, which are attached on both sides of the monopole array and terminated with loads. The mutual coupling effect between main elements is decreased due to coupling between dummy element and main element. Dummy elements can reduce the difference of the radiation pattern between each element of the monopole array. Therefore, our proposed scheme could improve the performance of the Doppler spread compensator.

5.2. Proposed Doppler Spread Compensator

Figure 5.1 illustrates the proposed Doppler spread compensator. It is composed of two dummy elements, which are placed on both sides of a monopole array. The antenna spacing between each element is d (λ is 0.6[m] when carrier frequency is 500MHz).

The space domain interpolator estimates a virtual reception point p, which is $x = vt$ apart from the first array element. Since p is stationary with respect to the ground, it can compensate for Doppler spread. To calculate p, the space domain interpolator requires vehicle speed information. In the following, I assume perfect knowledge of vehicle speed information.

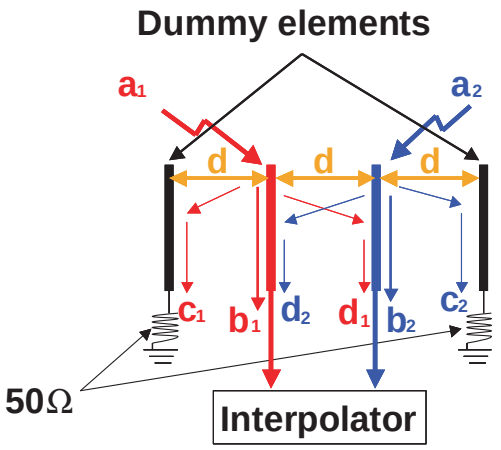

Figure 5.2. Effect of Dummy Elements

The received signal $\mathbf{r}(t) = [r_1 r_2]^t$ is applied to the space domain interpolator to estimate the received signal at position x,

$$\tilde{r}(t;x) \quad = \quad \mathbf{w}^H(x) \cdot \mathbf{r}(t) \tag{5.1}$$

where $\mathbf{w}(x)$ is a weight vector. The derivation of the weight vector is given in the Appendix A.

The output signal of the space domain interpolator is then applied to the OFDM receiver to demodulate the signal.

From Figure 5.2, dummy elements terminated with ground. The incoming waves $a1$ and $a2$, which are imputed to #1 and #2 elements, couple with each array element. The coupling signals $c1$ and $c2$, which couple between the dummy elements and the monopole array, are eliminated by dummy elements. Therefore, the mutual coupling effect between #1 and #2 elements, $d1$ and $d2$, can be reduced.

According to references [28, 12], mutual coupling affects the radiation pattern. The radiation pattern of an element in an array environment differs from the one in an isolated situation [28].

Dummy elements mitigate performance degradation due to the mutual coupling effect, because they can reduce the difference of the radiation pattern between each element of the monopole array.

5.3. Computer Simulation Results

To confirm the effectiveness of our proposed scheme, I carried out computer simulations. First, I analyzed complex value directivity of the monopole array using the moment method based on an antenna simulation tool, numerical electromagnetic code (NEC-2) [25]. The directivity patterns were applied to the fading simulator based on references [20, 26].

In the simulator, the amplitude and phase of each offset oscillator is adjusted according to the directivity.

Table 5.1 and Table 5.2 show antenna simulation parameters and computer simulation parameters, respectively.

Table 5.1. Antenna Simulation Parameters

Frequency	500MHz
Load Impedance	50Ω
Source	Incident Plane Wave
Antenna Length	0.25λ

Table 5.2. Computer Simulation Parameters

Transmission Parameters	
Bandwidth	5.572 MHz
Carrier Spacing	0.992 kHz
FFT size	8192
Number of Carriers	5617
Number of Data Carriers	4992
Carrier Modulation	64 QAM
Effective Symbol Duration	1.008ms
Guard Interval	126μs(1/8)
Propagation Model	
Model	Equal gain two-ray Rayleigh fading [20], GSM Delay Profile [26] (Hilly terrain 6-ray and 12-ray)
Direction of Arrival	Uniform distribution

In the computer simulation, I supposed Mode3 of ISDB-T standard, without error correction.

According to Appendix D, the optimum antenna spacing for the ideal monopole array is 0.075 λ, while the optimum antenna spacing for 2, 4 and 6-element monopole array with mutual coupling effect are 0.425λ, 0.25λ and 0.3λ, respectively at E_b/N_0=35dB and f_dT_s=0.1 (f_dT_s is the maximum Doppler shift frequency normalized by the effective symbol duration).

In the following simulation, I have made use of the optimum antenna spacing.

First, I investigated the radiation patterns of each main element. According to the reference [12, 28], radiation patterns of each main element are disturbed and the main elements will no longer be identical due to mutual coupling. Therefore, we can measure that the mutual coupling effect by comparing the radiation pattern of main elements. The smaller the radiation pattern difference is the less the degradation due to mutual coupling.

The radiation patterns are shown in Figure 5.3. The difference between the radiation patterns of 2-element monopole array is lager than that of 4 and 6-element monopole arrays. The difference between the radiation patterns of 6-element monopole is smaller than the other monopole arrays. It means that the mutual coupling effect of 6-element monopole array is less than the other monopole arrays. In the following, the computer simulation results show the proposed scheme is capable of improving BER performance by reducing mutual coupling effect.

Next, by using these radiation patterns, the computer simulation results show BER performance.

Figure 5.4 shows BER performance against f_dT_s, when E_b/N_0 is 35dB and is using the optimum antenna spacing. 'w/o compensator' means it does not employ Doppler spread compensator. The ideal monopole array, which has 2 elements and in which mutual coupling effect is not considered, gives better BER performance than a 6-element monopole array.

Figure 5.5 represents BER performance versus E_b/N_0, when f_dT_s is 0.1 and the optimum antenna spacing is used. The 2-element monopole array has a better BER performance than an ideal monopole array without a Doppler spread

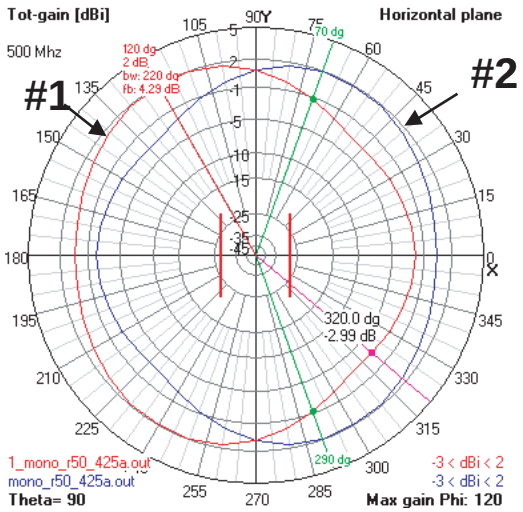

(a) 2-Element Monopole Array

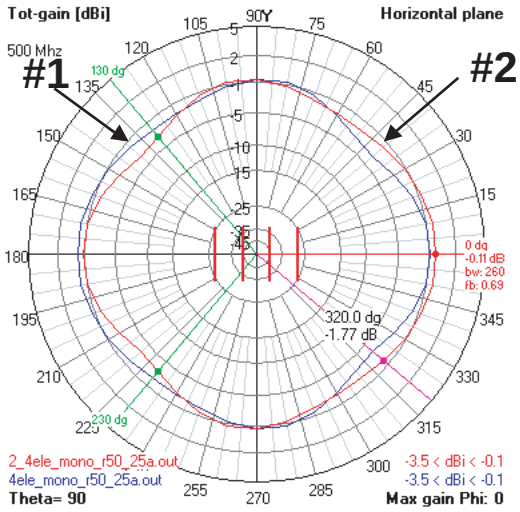

(b) 4-Element Monopole Array

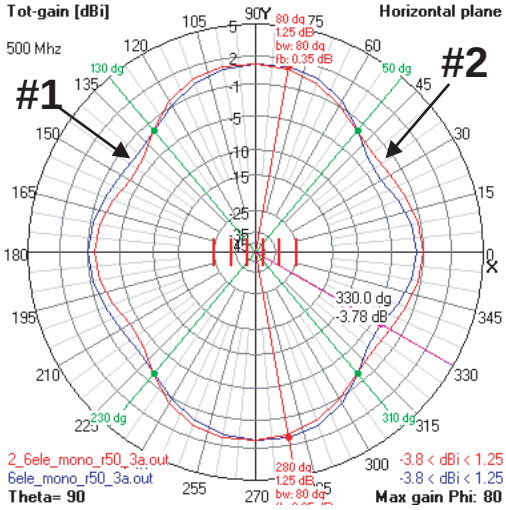

(c) 6-Element Monopole Array

Figure 5.3. Radiation Patterns (f_c = 500MHz, Antenna Length L = 0.15[m])

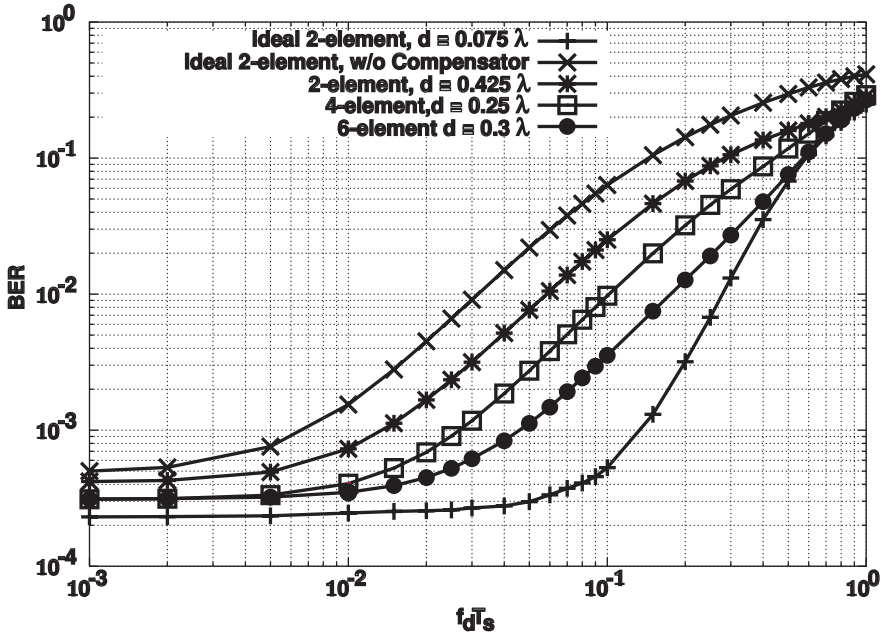

Figure 5.4. BER Performance against f_dT_s ($E_b/N_0 = 35$dB)

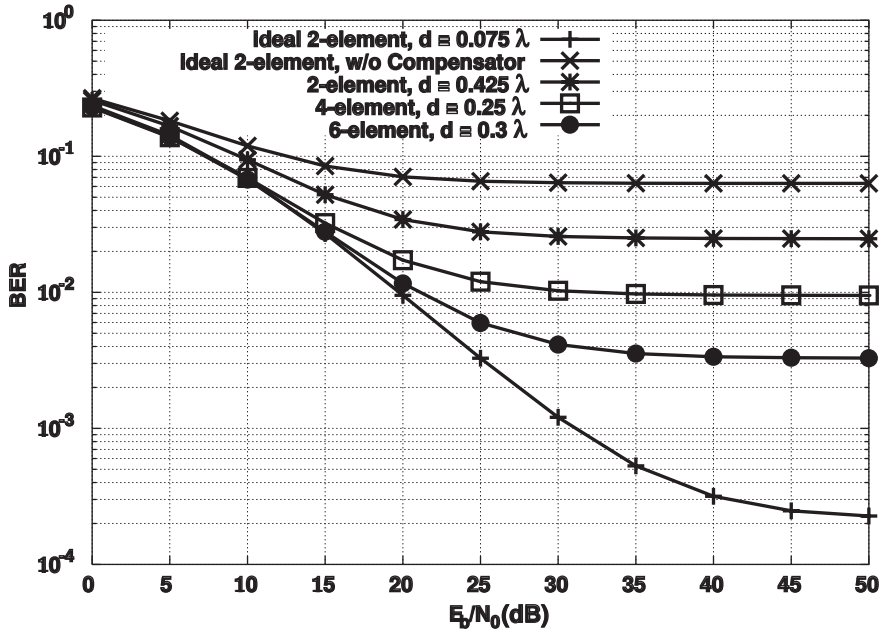

Figure 5.5. BER Performance against E_b/N_0 ($f_dT_s = 0.1$)

compensator. The 6-element monopole array gives better BER performance than a 2-element or 4-element monopole array.

The ideal monopole array, which has 2 elements and in which the mutual coupling effect is not considered, gives better BER performance than the 6-element monopole array.

According to Figures 5.4 and 5.5, 6-element monopole array has better BER performance than the other monopole arrays (2-element, 4-element) which consider the mutual coupling effect. We know that dummy elements effectively reduce the mutual coupling effect.

However, the proposed scheme takes much space due to the dummy elements. In Figure 5.6, it compares BER performance 4-element monopole arrays with dummy elements and without dummy elements. All the array elements are used for Doppler spread compensator in the case of 4-element monopole array without dummy elements.

From Figure 5.6, 4-element monopole array without dummy elements has better BER performance than 4-element monopole array with dummy elements. However, there is little difference in BER performance between 4-element monopole array with dummy elements and without dummy elements.

Figure 5.7 shows BER performance against carrier frequency, which is from 400MHz to 770MHz. '(x)' indicates the monopole array antenna is designed for 500MHz, while '(y)' indicates the monopole array is designed for 700MHz. The antenna spacing for 700MHz is obtained by optimization. The optimization result is given in Appendix D. Figure 5.7(a), 5.7(b) represent BER performance versus carrier frequency, when E_b/N_0 is 35dB and the vehicle speeds are 100 km/h and 200 km/h, respectively. In Figure 5.7(a) and 5.7(b), the vehicle speed is fixed as 100 km/h and 200 km/h, however, f_dT_s is changed because the carrier frequency is changed. On the other hand, in Figure 5.7(c), the maximum doppler shift frequency is fixed as 100 Hz regardless of the carrier frequency. The BER performance is deteriorated when vehicle speed is high.

From Figure 5.7, BER performance of the monopole array which is designed for 500MHz has deteriorated when carrier frequency is higher than 500MHz. Meanwhile, the monopole array which is designed for 700MHz has better BER performance than 500MHz.

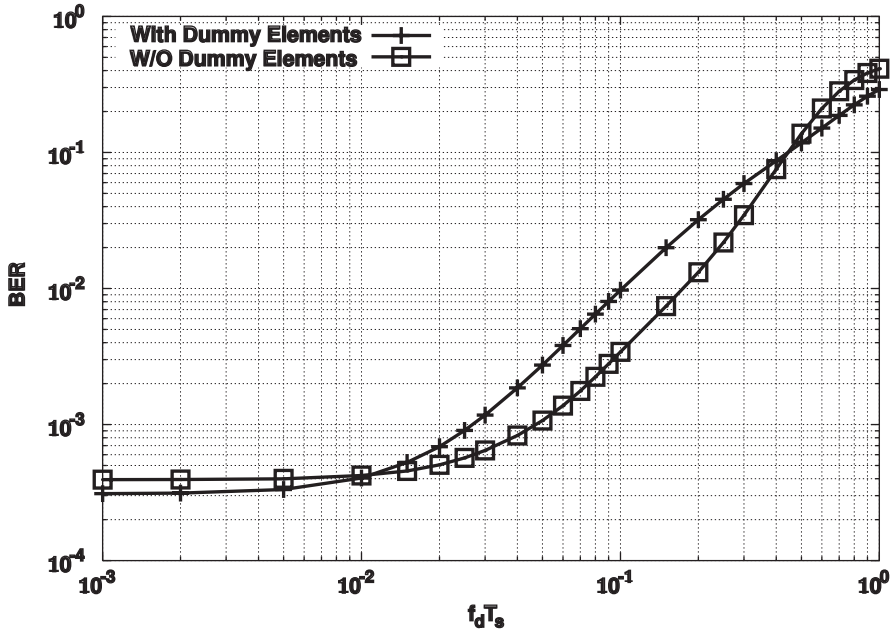

(a) BER Performance against f_dT_s, $E_b/N_0 = 35$dB

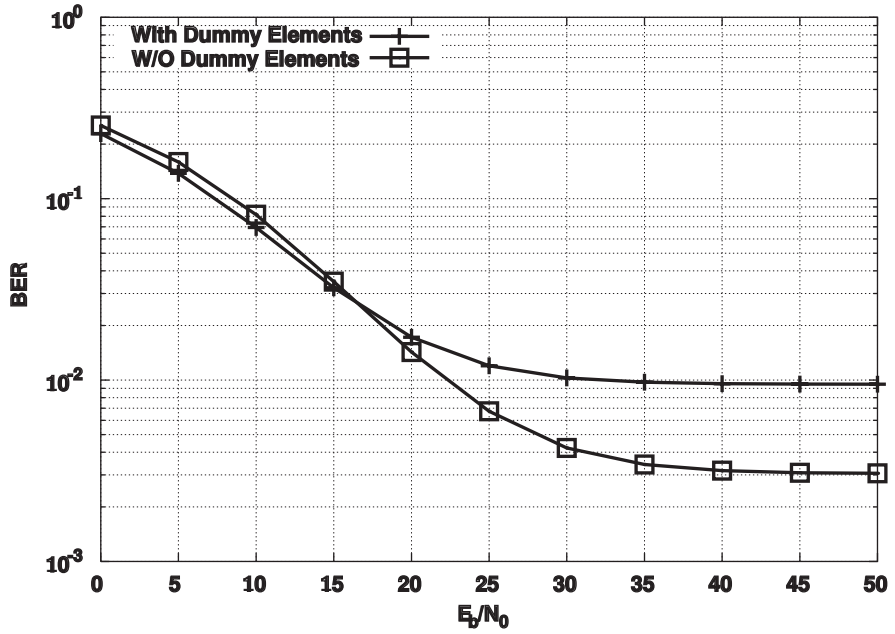

(b) BER Performance against E_b/N_0, $f_dT_s = 0.1$

Figure 5.6. BER Performance of 4-element with or without Dummy elements

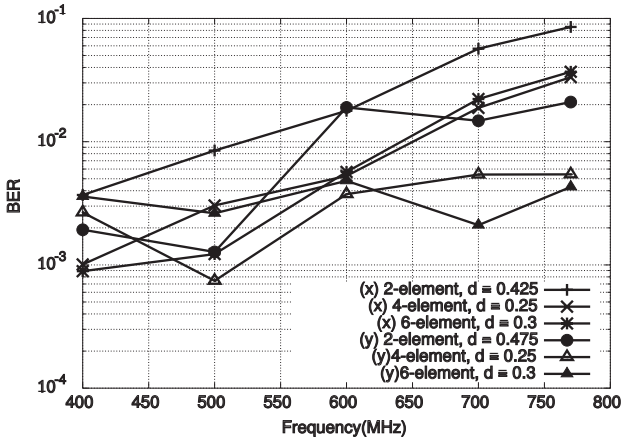

(a) Vehicle Speed, $v = 100km/h$

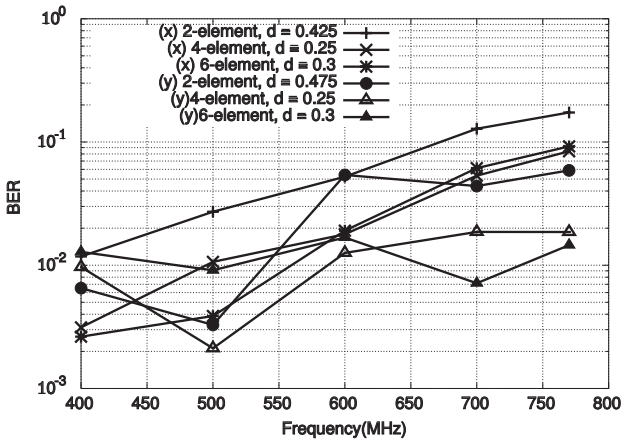

(b) Vehicle Speed, $v = 200km/h$

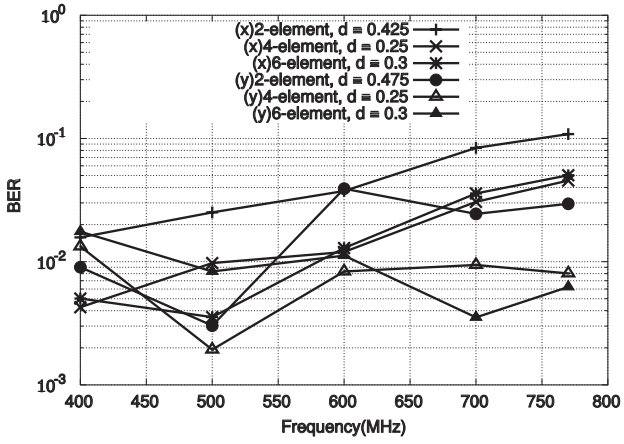

(c) $f_d T_s = 0.1$

Figure 5.7. BER Performance against Carrier Frequency ($E_b/N_0 = 35$dB)

On the other hand, 2-element monopole array for 700MHz gives better BER performance than 6-element monopole array for 700MHz when the carrier frequency is 500MHz. According to Figure 5.8, the radiation pattern difference of 2-element monopole array and 4-element monopole array is smaller than that for 6-element monopole array. Therefore, 2-element monopole array designed for 700MHz gives better BER performance than 6-element monopole array for 700MHz, when BER is measured at the carrier frequency of 500MHz.

The Operating bandwidth is the frequency region that the degradation due to mutual coupling is small enough for receiving the ISDB-T signal. As the required BER, I assume 2×10^{-2} before FEC when BER before inner code decoding is below 2×10^{-2}, a quasi error free (QEF) rate of 10^{-11} can be obtained after forward error correction (FEC) [29]. The receiver satisfies the required BER of 2×10^{-2} in the operating bandwidth region. The previously proposed method used mutual coupling canceller [10, 11], however, its operating bandwidth is 30MHz, which the total frequency band assigned for ISDB-T is 300MHz. It is difficult to design the mutual coupling canceller algorithm, which can compensate for throughout the ISDB-T band. On the other hand, the operating bandwidth of the monopole array with dummy elements for 700MHz is 370MHz. It is sufficient to cover ISDB-T bandwidth. Therefore, the proposed scheme provides wide operating bandwidth in order to add dummy elements on both sides of main elements.

Meanwhile, the monopole array with dummy elements which is designed for 700MHz has wide operating bandwidth irrespective of the vehicle speed.

Figure 5.9 shows BER performance of a monopole array versus various delay profiles. The delay profiles used the equal gain 2-ray Jakes model [20] and the hilly terrain 6-tap and 12-tap model of the global system for mobile communication (GSM) [26]. Figure 5.9(a) and Figure 5.9(b) show BER performance versus $f_d T_s$, when E_b/N_0 is 35dB, and BER performance against E_b/N_0, when $f_d T_s$ is 0.1, respectively.

According to Figure 5.9, although, the two-ray Rayleigh fading model is more severe environment than 6-ray and 12-ray models, the BER performance is similar in the three delay profiles. The reason is that delay of the two-ray fading model is within a guard interval. Also, our proposed dummy elements attached

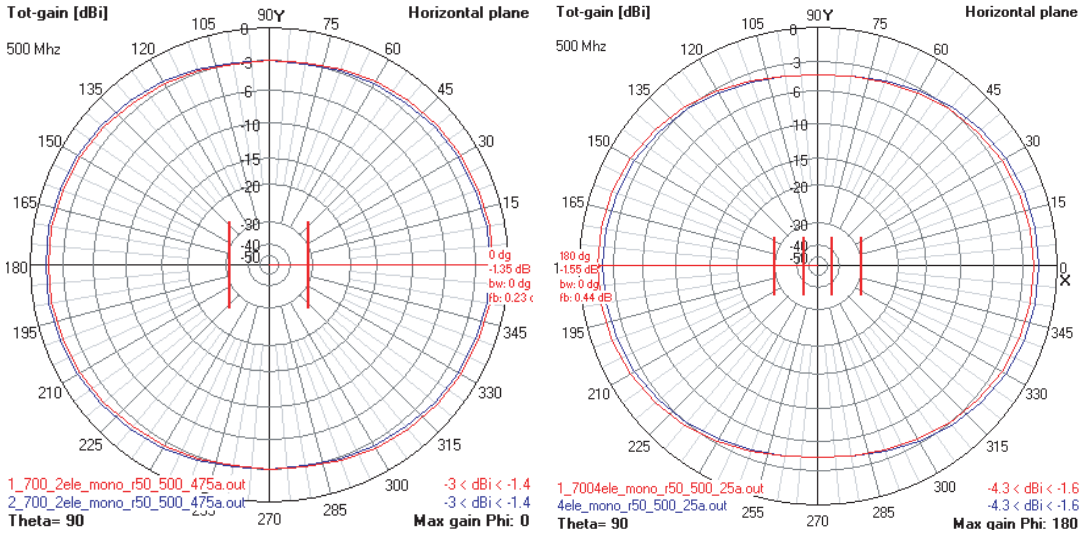

(a) 2-Element Monopole Array (b) 4-Element Monopole Array

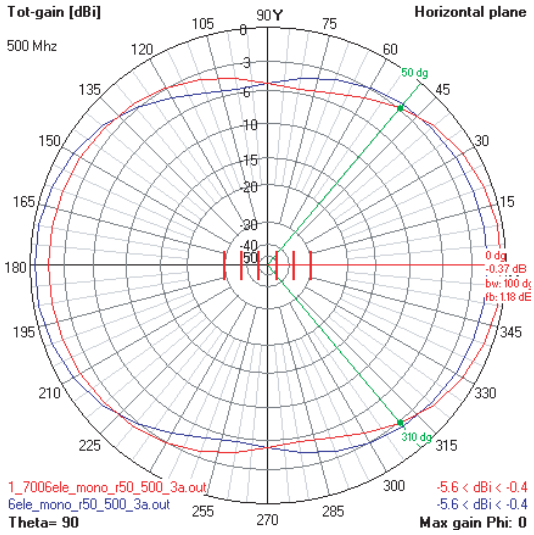

(c) 6-Element Monopole Array

Figure 5.8. Radiation Patterns (f_c = 500MHz, Antenna Length L = 0.107[m])

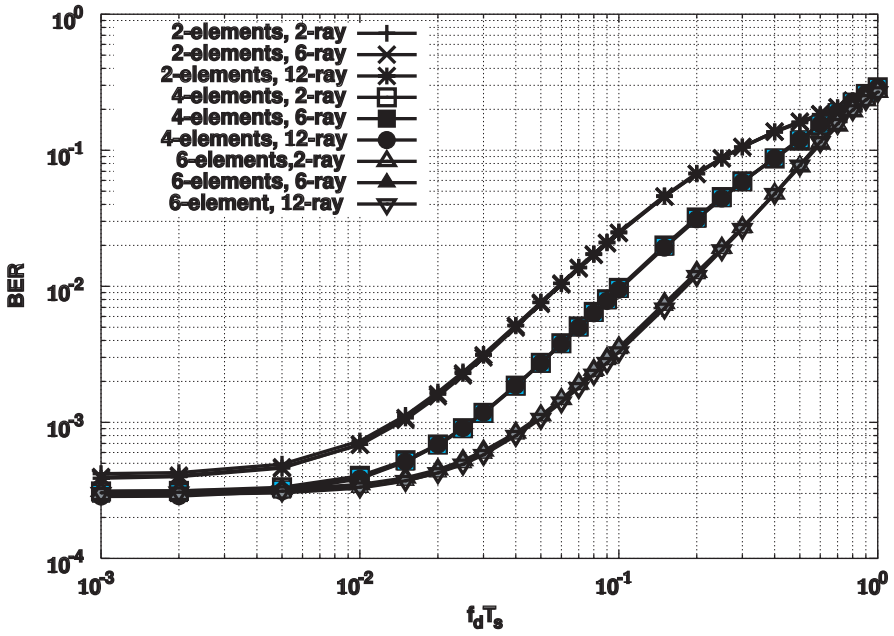

(a) BER Performance against f_dT_s ($E_b/N_0 = 35$dB)

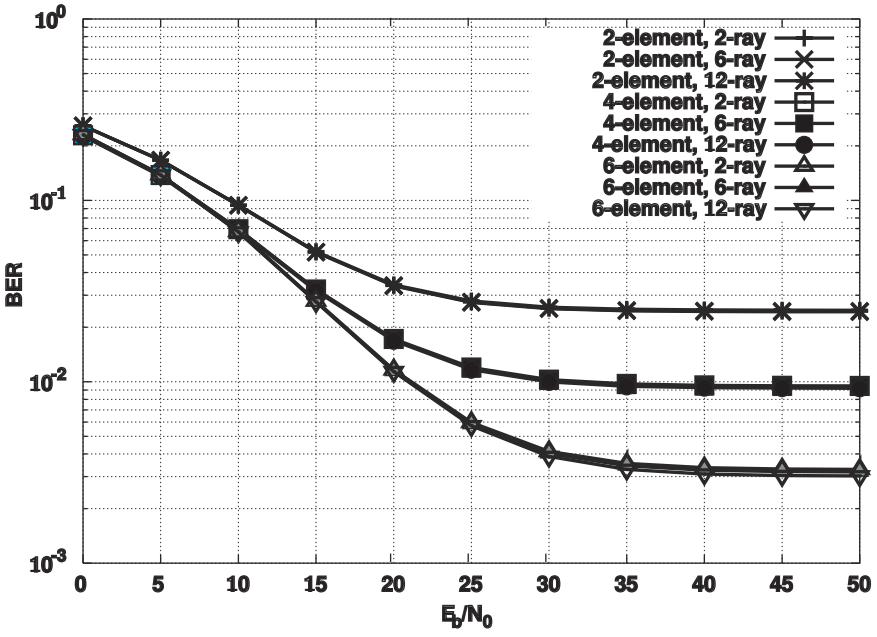

(b) BER Performance against E_b/N_0 ($f_dT_s = 0.1$)

Figure 5.9. BER Performance against Various Fading Models

on both sides of a monopole array give good BER performance in various mobile environments.

5.3.1 Mutual Impedance

The mutual resistance R_{21} and the mutual reactance X_{21} of 2-element monopole array can be expressed as in [30, 31] by

$$\begin{aligned}\mathbf{R}_{21} = \frac{15}{\sin^2(\beta L)}\Big[&2(2+\cos 2\beta L)\mathbf{Ci}\beta d - 4\cos^2\beta L\{\mathbf{Ci}\beta(\sqrt{d^2+L^2}-L)\\ &+\mathbf{Ci}\beta(\sqrt{d^2+L^2}+L)\} + \cos 2\beta L\{\mathbf{Ci}\beta(\sqrt{d^2+4L^2}-2L)\\ &+\mathbf{Ci}\beta(\sqrt{d^2+4L^2}+2L)\} + \sin 2\beta L\{\mathbf{Si}\beta(\sqrt{d^2+4L^2}+2L)\\ &-\mathbf{Si}\beta(\sqrt{d^2+4L^2}-2L) - 2\mathbf{Si}\beta(\sqrt{d^2+L^2}+L)\\ &+2\mathbf{Si}\beta(\sqrt{d^2+L^2}-L)\}\Big](\Omega),\end{aligned} \tag{5.2}$$

$$\begin{aligned}\mathbf{X}_{21} = \frac{15}{\sin^2(\beta L)}\Big[&-2(2+\cos 2\beta L)\mathbf{Si}\beta d + 4\cos^2\beta L\{\mathbf{Si}\beta(\sqrt{d^2+L^2}-L)\\ &+\mathbf{Si}\beta(\sqrt{d^2+L^2}+L)\} - \cos 2\beta L\{\mathbf{Si}\beta(\sqrt{d^2+4L^2}-2L)\\ &+\mathbf{Si}\beta(\sqrt{d^2+4L^2}+2L)\} + \sin 2\beta L\{\mathbf{Ci}\beta(\sqrt{d^2+4L^2}+2L)\\ &-\mathbf{Ci}\beta(\sqrt{d^2+4L^2}-2L) - 2\mathbf{Ci}\beta(\sqrt{d^2+L^2}+L)\\ &+2\mathbf{Ci}\beta(\sqrt{d^2+L^2}-L)\}\Big](\Omega),\end{aligned} \tag{5.3}$$

where L indicates antenna length, d means antenna spacing and β is $2\pi/\lambda$, λ being the wavelength of the transmitted carrier frequency. Also, cosine integral and sine integral is given by

$$\mathbf{Ci}(x) = \gamma + \ln(x) + \int_0^x \frac{\cos t - 1}{t} dt \tag{5.4}$$

$$\mathbf{Si}(x) = \int_0^x \frac{\sin t}{t} dt \tag{5.5}$$

where γ is Euler's constant 0.577215664. Consequently, the mutual impedance $\mathbf{Z}$

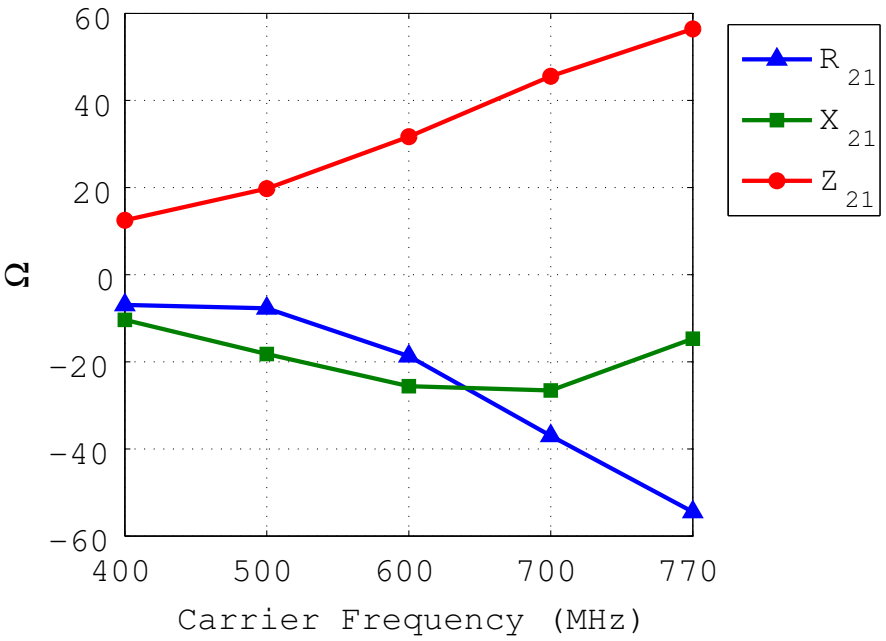

(a) Antenna Length L=0.15m, Antenna Spacing d=0.425λ(λ=0.6m)

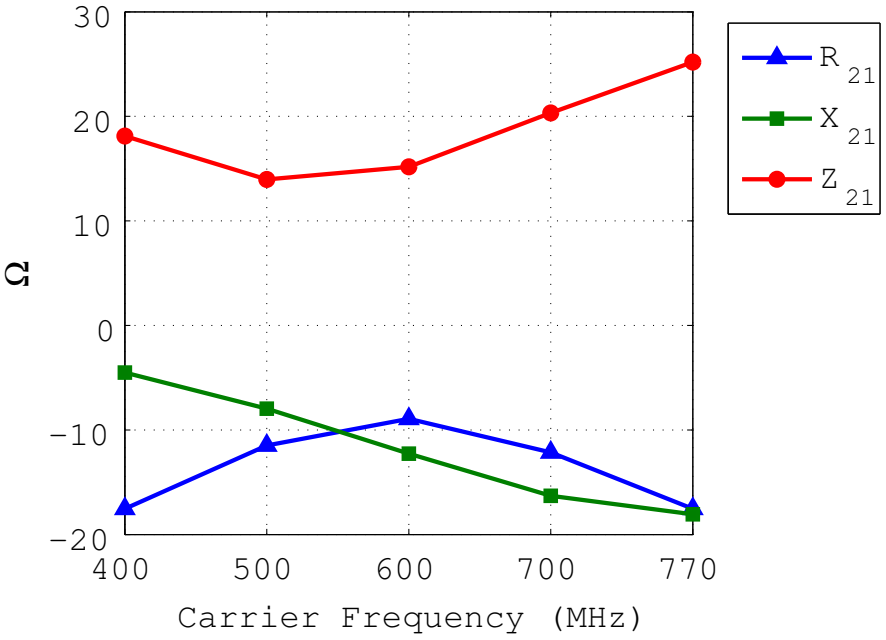

(b) Antenna Length L=0.107m, Antenna Spacing d=0.475λ(λ=0.428m)

Figure 5.10. Mutual Impedance against Carrier Frequency

is given by

$$\mathbf{Z} = \mathbf{R}_{21} + j\mathbf{X}_{21} \tag{5.6}$$

The mutual impedance of 2-element monopole array is shown in Figure 5.10, which is obtained by using equation 5.2, 5.3 and 5.6. Figure 5.10(a) shows the mutual impedance of 2-element monopole array which is designed for 500MHz against carrier frequency, where the antenna spacing d is 0.425λ. Also, the mutual impedance of 2-element monopole array which is designed for 700MHz against carrier frequency is shown in Figure 5.10(b), where the antenna spacing d is 0.475λ. From Figure 5.10, we know that the mutual impedance is increased in accordance with carrier frequency.

5.4. Conclusion

In this chapter, I have proposed dummy elements attached on both sides of a monopole array, which have an assisted Doppler spread compensator and a reduced mutual coupling effect. Also, they expand the operating bandwidth of a Doppler spread compensator.

The optimum antenna spacing was evaluated by computer simulation, and I then measured BER performance of our proposed dummy elements attached on both sides of a monopole array versus Doppler shift frequency, E_b/N_0, carrier frequency and various mobile environments. Also, the radiation pattern was evaluated by the antenna simulation tool NEC-2.

From antenna simulation results, I found that the difference in radiation patterns of each element becomes smaller if the number of dummy elements is increased. Therefore, the difference in radiation patterns of each element of a 6-element monopole array is smaller than other monopole arrays (2-element and 4-element).

According to computer simulation results, an ideal monopole array, which does not assume a mutual coupling effect, with a Doppler spread compensator has better BER performance than other monopole arrays (2-element, 4-element, 6-element). However, the BER performance of the 2-element monopole array,

which assumes mutual coupling effect, has deteriorated. If the number of dummy elements is increased, BER performance is improved.

Consequently, the proposed dummy elements attached on both sides of a monopole array effectively mitigate performance degradation due to the mutual coupling effect. They also expand the operating bandwidth of a Doppler spread compensator as well as having good BER performance in various mobile environments.

Chapter 6

Conclusion

This thesis introduced the performance improvement of ISDB-T receiver in fast fading environment. The bit error rate performance of the ISDB-T receiver drastically degrades due to multi-path fading and Doppler spread.

6.1. Dipole Array Assisted Doppler Spread Compensator with MRC Diversity

To mitigate performance degradation due to Doppler spread and multi-path fading simultaneously, dipole array antenna assisted Doppler spread compensator with MRC diversity for a mobile ISDB-T receiver was proposed. The proposed Doppler spread compensator estimates the received signal, which is not affected Doppler spread, by making use of each incoming signal from dipole array. MRC diversity was also adopted by using dipole array as a countermeasure of multi-path fading.

The optimum antenna spacing and spacing between reception points were determined by computer simulation. The optimum antenna spacing of the monopole array is $0.25[\lambda]$, while the optimum antenna spacing and the spacing between reception points of the dipole array are $0.325[\lambda]$ and $0.2[\lambda]$, respectively. I then have analyzed the BER performance of the proposed monopole array receiver and dipole array receiver by making use of the optimum antenna spacing and the spacing between reception points. According to the computer simulation results, the

proposed dipole array receiver has better BER performance than the monopole array receiver. Furthermore, to verify the validity of the proposed scheme, I analyzed how the BER performance of the proposed scheme was affected by the elevation angle of the incident wave. The vertically polarized monopole array receiver was not particularly affected by the elevation angle of the incident wave. However, the horizontally polarized dipole array receiver showed deterioration in BER performance when the standard deviation, σ, of the elevation angle was 10; however, it did not show high deterioration when the standard deviation was 0 to 5. The proposed dipole array receiver, which had better BER performance than the monopole array receiver, also had good BER performance regardless of the various propagation models.

6.2. Dummy Elements Method To Reduce Mutual Coupling Effect

In Chapter 5, dummy elements, which are attached on both sides of monopole array, method in order to mitigate performance degradation of Doppler spread compensator due to mutual coupling effect between main elements. Because dummy elements can reduce mutual coupling effect by coupling with main elements. Also, dummy elements method expands the operating bandwidth of a Doppler spread compensator. The performance of Doppler spread should be improved if it added more dummy elements, while it needs more space to set the array antenna.

The optimum antenna spacing was evaluated by computer simulation, and I then measured BER performance of our proposed dummy elements attached on both sides of a monopole array versus Doppler shift frequency, E_b/N_0, carrier frequency and various mobile environments. Also, the radiation pattern was evaluated by the antenna simulation tool NEC-2. From antenna simulation results, I found that the difference in radiation patterns of each element becomes smaller if the number of dummy elements is increased. Therefore, the difference in radiation patterns of each element of a 6-element monopole array is smaller than other monopole arrays (2-element and 4-element). According to the computer simulation results, an ideal monopole array, which does not assume a mutual coupling

effect, with a Doppler spread compensator has better BER performance than other monopole arrays (2-element, 4-element, 6-element). However, the BER performance of the 2-element monopole array, which assumes mutual coupling effect, has deteriorated. If the number of dummy elements is increased, BER performance is improved. Consequently, the proposed dummy elements attached on both sides of a monopole array effectively mitigate performance degradation due to the mutual coupling effect. They also expand the operating bandwidth of a Doppler spread compensator as well as having good BER performance in various mobile environments.

Throughout the results of this thesis, the proposed methods improve the performance of ISDB-T receiver in fast fading environment.

Appendix

A. Doppler Spread Compensator

The space domain interpolator uses a minimum mean square error (MMSE) algorithm. Let us assume the two-dimensional received signal vector $\mathbf{r}(t)$ as:

$$\mathbf{r}(t) = [r_1(t), r_2(t)]^T, \tag{1}$$

where $r_1(t)$ and $r_2(t)$ are the received signals from the first and the second array elements at time t. The output of the space domain interpolator, which estimates the received signal at the position x, is given by:

$$\tilde{r}(x,t) = \mathbf{w}^H(x)\mathbf{r}(t), \tag{2}$$

where $\tilde{r}(x,t)$ is the estimated signal at position x and $\mathbf{w}(x)$ is the weight vector, which uses the MMSE algorithm.

The weight vector, $\mathbf{w}(x)$, is given by:

$$\mathbf{w}(x) = \mathbf{R}^{-1}\mathbf{b}(x), \tag{3}$$

where $\mathbf{R}$ denotes the 2×2 correlation matrix of the received signal vector $\mathbf{r}(t)$ and $\mathbf{b}(x)$ is the 2-dimensional cross-correlation vector between the received signal vector and the desired signal $r(x,t)$. The correlation matrix is given by,

$$\mathbf{R} = \frac{1}{2}E[\mathbf{r}(t)\mathbf{r}^H(t)] \tag{4}$$

where,

$$R_{n,k} = J_0(2\pi d(n-k)/\lambda) \quad (5)$$

is the n-th column, k-th row element of $\mathbf{R}$. $(n, k \in \{1, 2\})$ The cross correlation vector is also given by,

$$\mathbf{b}(x) = \frac{1}{2}E[\mathbf{r}(t)r(x,t)^*] \quad (6)$$

where,

$$b_k(x) = J_0(2\pi(kd-x)/\lambda) \quad (7)$$

is the k-th $(k = 1, 2)$ element of $\mathbf{b}$. In the above equations, $\mathbf{x}^H$ represents the Hermitian transpose of $\mathbf{x}$ and $x^*$is the complex conjugate of x. $J_0(x)$ is the zero-th order Bessel function of the first kind.

B. Interpolation and Extrapolation

I considered two types of offset values, x_{off1} and x_{off2}, as shown in Figure 1. In the case of Type 1, x_{off1} is set to be zero and x_{max2} be $a\lambda$. Doppler spread compensator estimates the virtual reception point where is between the array elements. That is, Doppler spread compensator only can do interpolation. In hence, performance of Doppler spread compensator is improved when the vehicle is moved high speed. However, in this case, the diversity gain is decreased because Doppler spread compensator needs narrow antenna spacing.

On the other hand, Doppler spread compensator estimates the virtual reception point where is between array elements and outside of array elements in Type 2. That is, Doppler spread compensator can do interpolation and extrapolation. Since, the antenna spacing is wider than Type 1, diversity gain is increased when the vehicle runs high speed. As shown in Figure 2, Type 2 has better BER performance than Type 1 when E_b/N_0 is 20[dB] and the antenna spacing d and a are 0.325λ, 0.2λ, respectively. Therefore, the proposed Doppler spread compensator uses offset values of Type 2.

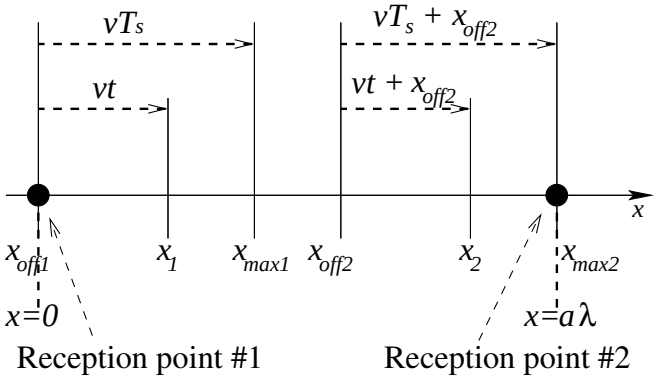

(a) Type 1

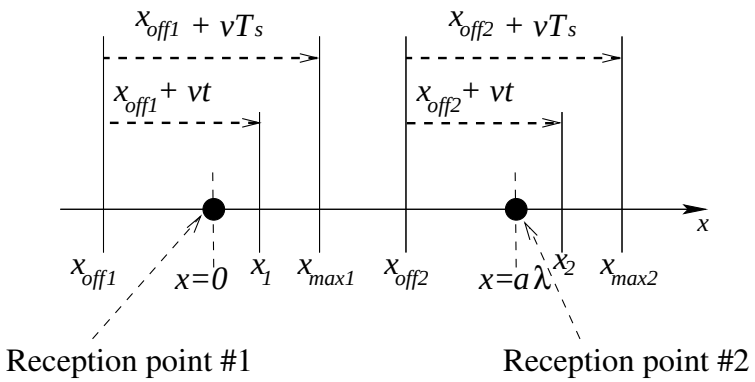

(b) Type 2

Figure 1. Configuration of Offset value

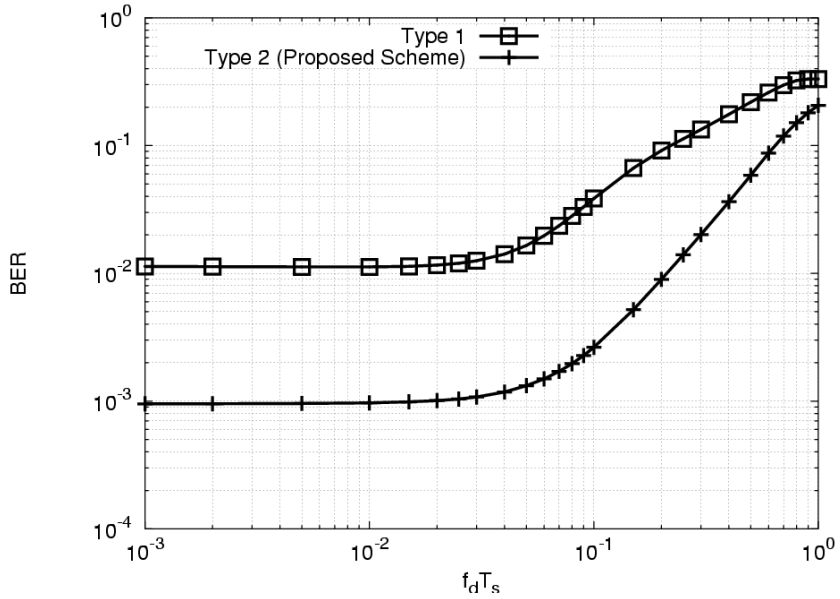

Figure 2. BER performance against f_dT_s, when E_b/N_0 is 20dB and $d = 0.325\lambda$, $a = 0.2\lambda$

C. Maximum Ratio Combining Diversity

In maximum ratio combining (MRC) diversity, each branch signal is weighted and combined in order to improve signal to noise ratio (SNR). In this thesis, the post-FFT (Fast Fourier Transform) MRC diversity method is employed. The received signals, received from each branch, are weighted then combined as shown in Figure 3. The combined signal is

$$g = \sum_{i=1}^{K} w_i r_i \tag{8}$$

where w_i is weight value of each branch and r_i is the received signal of each branch. The total noise power is the sum of the noise powers in each branch:

$$N_T = N \sum_{i=1}^{K} w_i^2 \tag{9}$$

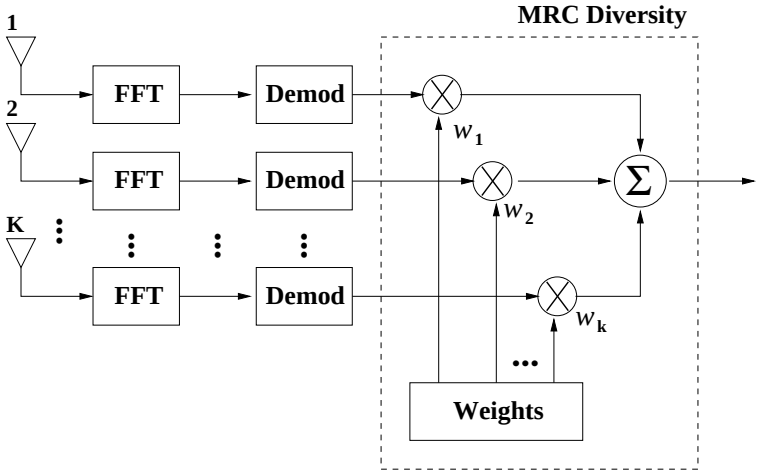

Figure 3. Post-FFT MRC Diversity Receiver

where the mean noise power per branch $\overline{n_i^2}$ be the same for all branches, $\overline{n_i^2} = N$. The SNR of the combined signal is

$$\gamma = \frac{g^2}{2N_T} \tag{10}$$

In order to obtain the maximum γ, the weight value should be defined as follows

$$w_i = r_i/\overline{n_i^2} \tag{11}$$

If the weight values, w_i, are chosen as stated above, then the SNR of the combined signal will be maximized with a value

$$\begin{aligned} \gamma &= \Big(\sum_{i=1}^{K} r_i^2/N\Big)^2/2N\sum_{i=0}^{K}(r_i/N)^2 \\ &= \sum_{i=1}^{K}\frac{r_i^2}{2N} \\ &= \sum_{i=1}^{K}\gamma_i \end{aligned} \tag{12}$$

Therefore, the SNR of combiner output is the sum of the SNR of the individual branches.

However, to implement MRC diversity, the weight values need both amplitude and phase tracking of the channel response. Moreover, linear amplifiers and phase shifters over a large dynamic range of input signals are needed [19].

The probability density function of γ is given by

$$p(\gamma) = \frac{\gamma^{K-1} e^{-\gamma/\Gamma}}{\Gamma^K (K-1)!} \tag{13}$$

where all branches have equal mean SNR $\Gamma_i = \Gamma$. The probability distribution function of γ is given by integrating the density function,

$$\begin{aligned} P_K(\gamma) &= \frac{1}{\Gamma^K (K-1)!} \int_0^\gamma x^{K-1} e^{-x/\Gamma} dx \\ &= 1 - e^{-\gamma/\Gamma} \sum_{i=1}^{K} \frac{(\gamma/\Gamma)^{i-1}}{(i-1)!} \end{aligned} \tag{14}$$

The probability distribution function, $P_K(\gamma)$, is plotted in Figure 4. At 99% reliability MRC diversity provides a 12dB savings in power with two branches and 19dB savings with four branches.

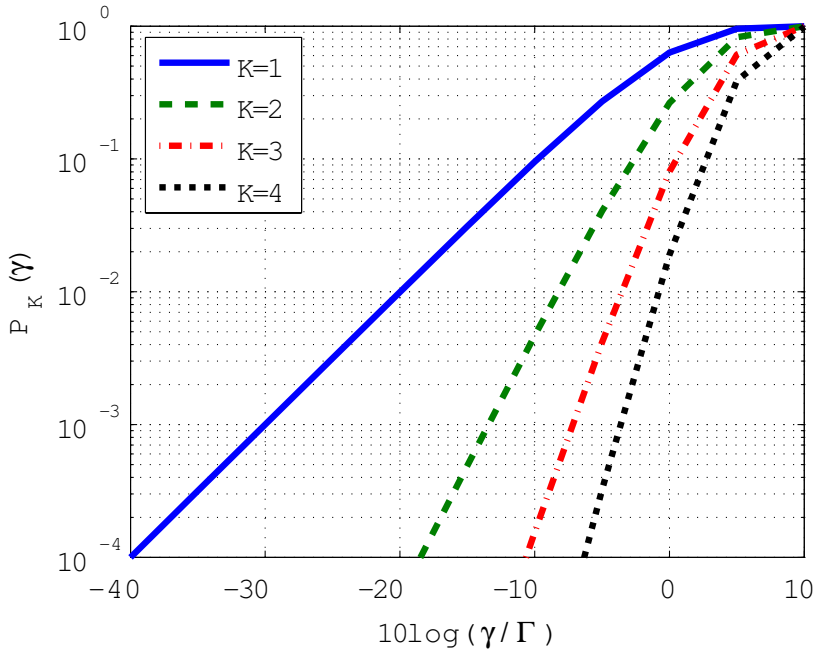

Figure 4. Probability distribution of SNR, γ, for K-branch MRC diversity combiner. (Γ is SNR on one branch)

D. Optimization Results of Dummy Elements Method against the Antenna Spacing

The optimum antenna spacing, which minimizes BER, is obtained by computer simulation, which uses Jake's fading model [20], that is, there are many incoming paths, where direction of arrivals are uniformly distributed.

Figure 5(a), 5(b) and 5(c) show BER performance versus antenna spacing $d\lambda$, when E_b/N_0 is 35dB, carrier frequency is 500MHz and f_dT_s is 0.05, 0.1 and 0.15, respectively. According to Figure 5, the optimum antenna spacing d of 2-element monopole array is 0.425 λ; and 4-element monopole array, which has 2 dummy elements on both sides of monopole array, is 0.25 λ. Also, the optimum antenna spacing of a 6-element monopole array, which has 4 dummy elements on both sides of monopole array, is 0.3 λ. In the case of the ideal monopole array, the optimum antenna spacing d is changed in accordance with f_dT_s. The optimum

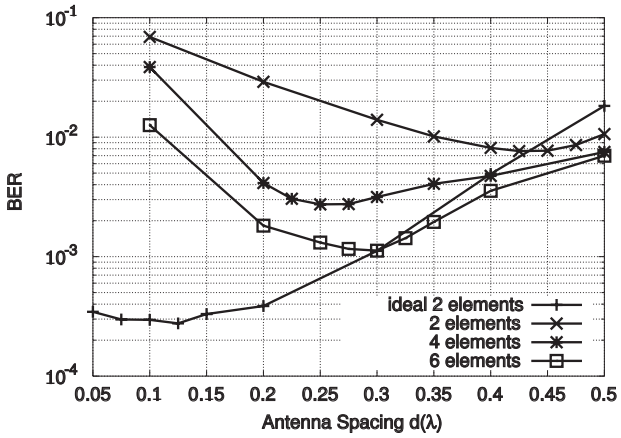

(a) $f_d T_s = 0.05$

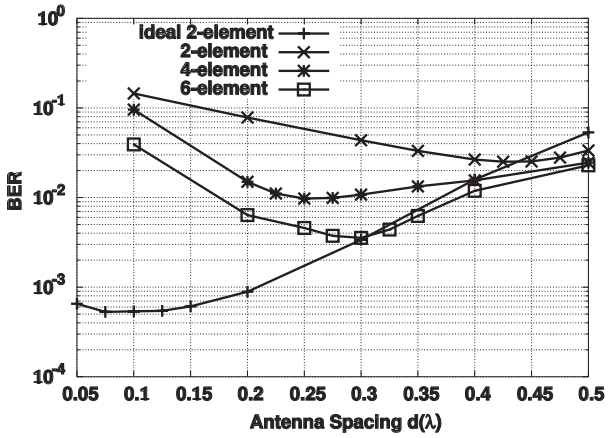

(b) $f_d T_s = 0.1$

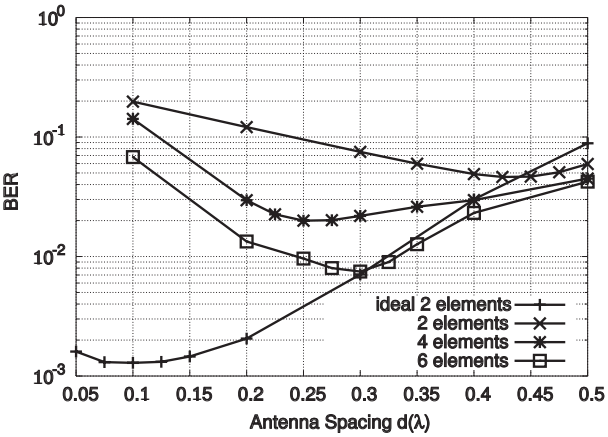

(c) $f_d T_s = 0.15$

Figure 5. Optimization vs. Antenna Spacing ($E_b/N_0 = 35$dB, $f_c = 500$MHz)

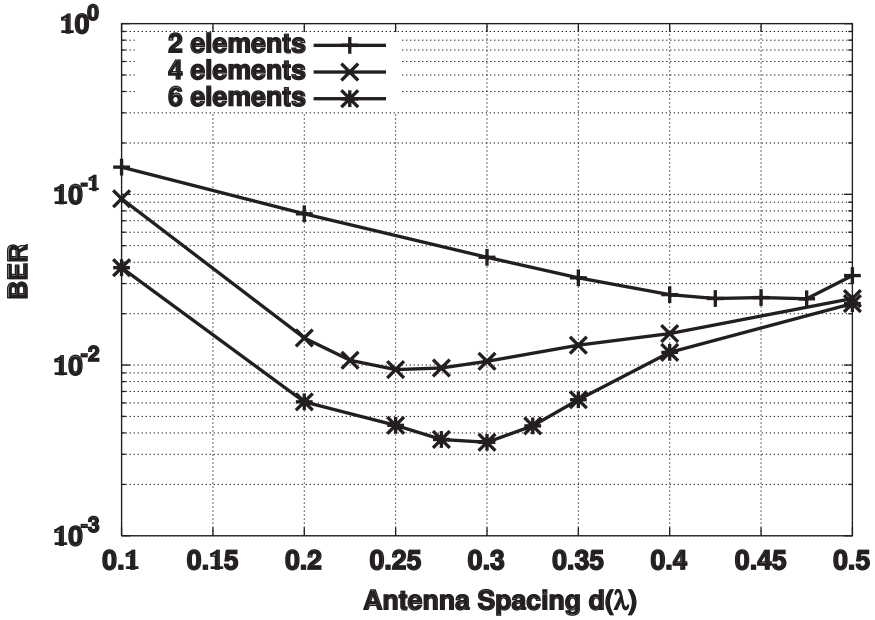

Figure 6. Optimization vs. Antenna Spacing($f_dT_s = 0.1$, $E_b/N_0 = 35$dB, $f_c =$ 700MHz

antenna spacings of ideal monopole array are 0.125 λ, 0.75 λ and 0.1 λ when f_dT_s is 0.05, 0.1 and 0.15, respectively. However, the difference in antenna spacing gives little impact on the BER performance.

The optimum antenna spacing with mutual coupling is shown in Figure 6 when f_dT_s is 0.1, E_b/N_0 is 35dB and carrier frequency is 700MHz. The optimum antenna spacing of 2-element monopole array is 0.475 λ, 4-element monopole array is 0.25 λ and 6-element monopole array is 0.3 λ, respectively. In this case, λ is expressed wavelength at 700MHz and the value is approximately 0.428 m.

According to Figure 5 and 6, the BER performance became worse even mutual coupling is reduced by extending the antenna spacing. The reason is that the received signals from the array elements should be correlated with each other in order to estimate the received signal at a certain reception point between two elements. Therefore, performance of the Doppler spread compensator has deteriorated if the antenna spacing reaches 0.5 λ, even if it could reduce mutual coupling effect.

On the other hand, if the antenna spacing is narrow, performance of the

Doppler spread compensator has deteriorated due to mutual coupling effect while the correlation between two signals grows. In the case of the ideal monopole array simulation, it does not take into account the effect of mutual coupling but the correlation between array elements is considered.

There is a trade-off between the correlation and mutual coupling. In order to satisfy the both condition, we have to set the antenna spacing to minimize the BER as shown in Figure 5 and 6. The Doppler spread compensator, which uses the optimum antenna spacing, should have good BER performance in fast fading environment. Besides, the proposed scheme prevents the Doppler spread compensator performance degradation due to mutual coupling effect in fast fading environment. Therefore, the optimum antenna spacing has validity in fast fading environment.

References

[1] Information Technology – Generic coding of moving pictures and associated audio information Systems, ISO/IEC 12818-1:2000, JTC 1/SC 29; ISO Standards.

[2] ATSC Digital Television Standard (A/53) Revision E, with Amendments No. 1 and 2; Advanced Television Systems Committee Doc.A/53E, December 2005.

[3] Digital Video Broadcasting (DVB) for terrestrial televison; ETSI standard EN 300 744 Vol. 1.4.1, January 2001.

[4] Transmission for digital terrestrial television broadcasting, ISDB-T; ARIB standard STD-B31 Vol. 1.5.

[5] Radio Broadcasting Systems; Specification of the video services for VHF Digital Multimedia Broadcasting (DMB) to mobile, portable and fixed receivers; TTA standard TTAS.KO-07.0026.

[6] IEEE 802.11 WEB URL:http://grouper.ieee.org/groups/802/11/.

[7] Y. Jiang, X. Gao, and X. You, "Frequency Offset Estimation for OFDM Systems with a Novel Frequency Domain Training Sequence", IEICE Trans. Commun., Vol. E89-B, No. 4, pp.1194 - 1204, April 2006.

[8] P.S. Wijesena, and Y. Karasawa, "Beam-Space Adaptive Array Antenna for Suppressing the Doppler Spread in OFDM Mobile Reception", IEICE Trans. Commun., Vol. E87-B, No. 4, pp.20 - 28 January 2004.

[9] S.A. Husen, and S. Baggen, "Simple Doppler Compensation for DVB-T", 9th Int. OFDM-Workshop 2004, pp.67 - 71 September 2004.

[10] M. Okada, H. Takayanagi, and H. Yamamoto, "Array Antenna Assisted Doppler Spread Compensator for OFDM", ETT, Vol. 13, No. 5, September/October 2002.

[11] M. Okada, H. Takayanagi, and H. Yamamoto, "Array Antenna Assisted Doppler Spread Compensator for Mobile Reception of Terrestrial Television Broadcasting", Journal of Institute of Image Information and Television Engineers, Vol. 56, No. 2, pp.237 - 244, February 2002.

[12] S. Lundgren, "A study of Mutual Coupling Effects on the Direction Finding Performance of ESPRIT with a Linear Microstrip Patch Array Using the Method of Moments", IEEE Antennas and Propagation Society International Symposium, Vol. 2, pp.1372 - 1375, July 1996.

[13] B. Lindmark, "Comparison of Mutual Coupling Compensation to Dummy Columns in Adaptive Antenna Systems, IEEE Trans. on Antennas and Propagation", Vol. 53, No. 4, April 2005.

[14] http://www.dvb.org.

[15] R. V. Nee, and R. Prasad, "OFDM for Wireless Multimedia Communications", Boston: Artech House Publishers, Chapter 1, 2000.

[16] "Channel Coding, Frame Structure and Modulation Scheme for Terrestrial Integrated Services Digital Broadcasting (ISDB-T)", ITU-R Recommendation 11A/JxxE, 1999.

[17] Digital Audio Broadcasting (DAB); ETSI standard EN 300 401, 2nd Edition, May 1997.

[18] Clake R.H., "A Statiscal Theory of Mobile Radio Reception", Bell System Tech. J., Vol. 47, No. 6, pp.957 - 1000, July-August 1968.

[19] Lal Chand Godara, "Handbook of Antennas in Wireless Communications", CRC Press, 2002.

[20] W. Jakes, "Microwave Mobile Communications", IEEE Press, 1974.

[21] S. O. Rice, "Mathematical Analysis of Random Noise", Bell System Tech. J. Vol. 23, pp.282 - 332, July, 1944.

[22] S. O. Rice, "Statistical Properties of a Sine Wave Plus Random Noise", Bell System Tech. J. Vol. 27, pp.109 - 157, January, 1948.

[23] T. Wada, M. Okada, and H. Yamamoto, "Novel Array Antenna Assisted Adaptive Modulation Scheme for Fast Fading Channel", IEICE Trans. Commun., Vol. E88-B, No. 8, pp.3383 - 3392, August 2005.

[24] M. Okada and S. Komaki, "Random FM Noise Compensation Scheme for OFDM", Electronics Letters, Vol. 36, No. 19, pp.1653 - 1654, September 2000.

[25] http://www.nec2.org/.

[26] ETSI GSM recommendation 05.05, Annex C, 1994.

[27] C. B. Dietrich, K. Dietze, J. Randle Nealy, and W. L. Stutzman, "Spatial, Polarization, and Pattern Diversity for Wireless Handheld Terminals", IEEE Transactions on Antennas and Propagation, Vol. 49, No. 9, pp.1271 - 1281, September 2001.

[28] Hubregt J. Visser, "Array and Phased Array Antenna Basics", England: Wiley, Chapter 11, pp.295 - 298, 2005.

[29] "Terrestrial Digital Television Broadcasting", Broadcast Technology no.20, NHK STRL, Autumn 2004.

[30] G. H. Brown and R. King, "High Frequency Models in Antenna Investigations", Proc. IRE, Vol. 22, No. 4, pp.457 - 480, April 1934.

[31] John D. Kraus, "Antennas", 2nd Edition, USA: McGraw-Hill, Chapter 10, pp.426 - 427, 1998.